POLITECNICO DI TORINO

Master degree course in Electronic Engineering

Master Degree Thesis

Indoor human localization: a sensor fusion approach using long distance capacitive and infrared sensors

Supervisors
prof. Mihai Teodor Lazarescu
prof. Luciano Lavagno

Candidate
Irene Castro
ID:242266

Accademic Year 2019-2020

"Gutta cavat lapidem, non vi sed sæpe cadendo."
Dripping water hollows out stone, not through force but through persistence
Lucretio, De rerum natura

Summary

The possibility to have a reliable system that detects the exact position of a human in a room arouses a lot of interest since it could lead to numerous improvements in everyday life. Fields of application range from smart homes, where indoor human localization can be used for adjusting the lights or the heating in user's proximity, to hospitals and hospices where it can help to monitor patients remotely. For these and more other applications, a growing interest in this field has developed during the last years.

In this context, a research team at the Department of electronics and telecommunications (DET) of Politecnico di Torino is working to design a low cost, easy to use, unobtrusive, passive, tag-less and privacy-aware indoor localization system that can be safely and easily installed in smart homes and assisted living environments by using long-range capacitive sensors, digital filters and neural networks. Within this project this thesis work has the purpose of improving the performance, reliability and accuracy of the overall system by implementing a complementary sensor fusion technique between the existing capacitive sensors network localization system and an infrared thermal sensor localization system designed for this scope.

At the beginning of this thesis work, a study of the state of art on indoor human localization has been carried out. The advantages and disadvantages of the analyzed systems have been identified and a comparison among them has been made. From this analysis, it emerged that, even though the infrared and capacitive sensors have not the best accuracy among all the systems analyzed, their accuracy can be sufficient for indoor localization purpose. Moreover, both of them are cheap, safe, tagless, do not consume much power and are privacy-aware. Moreover, most of the weak points of these two techniques are complementary.

The main problem of capacitive sensors lies in the fact that they have a sensitivity that steeply decreases with the increase of distance from them. Furthermore, they are affected by different sources of noise that cannot be easily controlled. Above all, drift affects most this kind of sensor. On the

other hand, the infrared thermal sensor is affected by kinds of noise that are often complementary to the ones affecting capacitive sensors. For this reason, a sensor fusion between the two has been implemented.

During the experimental part of this thesis, the design of the infrared sensor system has been made. Going into detail, a MEMS Thermal Sensor has been chosen for the complementary acquisition system. It uses the thermopile technique in order to give information about the surface temperature of an object in an array of 16 pixels (4x4). By attaching it on the ceiling of a room, when a human passes underneath the sensor inside that area, it detects him/her as a higher temperature pixel with respect to the floor temperature, allowing to detect user's position and respecting the privacy.

Data from the infrared sensor have been collected using as microcontroller an Arduino Uno board using I2C communication protocol. Reliability of data has been improved by checking the integrity of the received data using the CRC-8 (Cyclic Redundancy Check) and by requesting to re-send in case of error. The samples collected on the board have been sent via radio to a second Arduino Uno board connected to a computer. For this reason, two Xbee modules have been programmed, one used as transmitter and the other as receiver.

The output wave signals from the sensor have been analyzed with an oscilloscope to choose the maximum reliable sampling rate for the infrared sensor system, that turned out to be 8 Hz. Data processing and packing have been made using the software MATLAB. For each set of data, a heat-map of the room has been plotted to have a graphical representation of data. The system has been tested and a stability characterization has been carried out by comparing the output temperature from the infrared sensor with a reference DTH11 Humidity Temperature Sensor. It has been observed that the difference between the values read from the sensors changed in synchrony with the DHT11 sensor.

The operation of each of the four capacitive sensor nodes has been tested separately. In particular, a sensitivity test has been made by moving in front of each sensor in a straight line, starting from a distance of 1.8 meters and approaching each time by a small step of 30 centimetres and recording the data acquired. The test has been repeated in different conditions, by changing the location of the sensors in the room, by changing some electronic components of the circuit and re-soldering some contacts. In the end, an increment of the sensitivity and a reduction of high-frequency noise have been obtained for most sensor nodes.

After testing all system components separately, a complete experiment has

been set up. In addition to the two systems described, an ultrasound sensor network has been installed to have an accurate reference for the position of the person in the room. This system is composed by a network of 4 stationary ultrasonic beacons and a mobile beacon - called hedgehog - worn by the person to be tracked. The room used for the experiment is a 3 m x 3 m room with a ceiling at a height of 3.05 m. In this structure, capacitive sensor plates are placed at the centre of the walls at a height of 120 cm from the floor, the infrared sensor is placed at the central point of the ceiling and the ultrasound sensors are placed at the four edges of the ceiling and communicate with a tag on the person's head.

Data from all sensors have been acquired simultaneously and the obtained results have been analyzed. Considering the factors that could positively and negatively influence the reading of the data by the capacitive and infrared sensors, different experiments have been carried out under different conditions. In particular, experimental data were collected in four experiments executed by two different people and lasted half an hour each. During these experiments, the person was slowly and continuously walking inside the room while all three localization systems were active. The first two experiments (one for each person) were carried out in the evening after sunset, while the other two during the afternoon with the sun's rays penetrating the room through blinds. It was, therefore, possible to test the system under different temperature conditions and with and without the interference of sunlight in the room. In the third experiment, an element of disturbance to the infrared system has been inserted to better test the sensor fusion technique.

From experimental results has been observed that by merging the data from the two sensing systems a much more accurate, sensitive and robust system can be created. Capacitive drift can be corrected by using the infrared sensor since it is not affected by the same problem. The overall sensitivity range can be extended for both the systems: the lack of sensitivity of the infrared sensor at the borders of the room are balanced by the high sensitivity of the capacitive sensors in the proximity of the walls. In the same way, the lack of sensitivity of the capacitive sensors in the middle point of the room is compensated by the field of view area of the infrared one. In the parts where both systems have good sensitivity, the infrared non-homogeneous sensitivity when crossing pixels can be corrected by the capacitive ones.

To check the improvement obtained, it will be necessary to analyze the data through Neural Networks by comparing the localization performance using first the data-set composed by data from only capacitive sensors, then only data from infrared sensors and at last a merge of the two systems. In this

way, it will be clear in terms of accuracy and error the actual improvement that the sensor fusion can give to both the systems.

During this work, a lot of effort has been made to make everything work in the best way and to try to have a scientific approach to the problems encountered. The expectation is that this system will be enhanced for improving the lives of users, especially those who need care and assistance.

Contents

List of Tables

List of Figures

Chapter 1

Introduction to Indoor Human Localization

1.1 Importance of indoor human localization and its fields of use

Nowadays technology is increasingly present in our lives: the furniture in our homes becomes increasingly smarter and interacts with us, robots are replacing us in carrying out a lot of works, even in the assistance and monitoring of people in need of care. In this context to localize people inside a closed environment arouses a lot of interest.

The possibility to have a reliable system that detects the exact position of a human in a room could lead to numerous improvements in everyday life.

Starting from trivial applications, indoor human localization can be used in smart homes for predicting the needs of the inhabitants based on their location and movements. For example, an automatic system can be programmed for adjusting the lights or the heating in the proximity of the person; a distributed sound system could use this information to follow the user as he moves among the various rooms. This can be useful to reduce the waste of energy, switching off some electronic devices when the user is not near them. Moreover, an indoor localization system makes it possible to detect the presence of intruders in the house and to activate an alarm system.

Inside a museum, the position of the user could be used for giving him contextualized contents about the artwork he is looking at through audio guides.

In the entertainment field, video-games could take advantage of the position of the player, for example, to move its avatar in a virtual world.

Considering also other application domains, indoor human localization can play an essential role in improving the quality of life of people with health problems. It would be for example a huge help for people with visual impairments, who could benefit from this technology succeeding in finding the way even in unknown places.

In hospitals and hospices or even in the houses of sick or elderly people, a localization system can help monitor patients remotely.

In the industry field, a reliable indoor location system could be used for the full automation of employees' work and to prevent accidents, increasing both productivity and safety.

Summing up, the indoor human localization can be useful for making life easier, more comfortable, smarter and even safer. Considering all these advantages, it is understandable the increasing interest in this field.

1.2 Characteristics of an ideal indoor human localization system

In the last years, various technologies have been developed to detect the presence of people in closed environments.

Global Navigation Satellite Systems (GPS or GNSS), the most used technology for localization in external environments, is instead useless inside buildings, both for the lack of precision and for the architectural barriers that prevent the signal from passing. In fact, GPS relies on radio transmissions in the spectrum of microwaves (on frequencies close to 1500 MHz) that suffer a heavy absorption phenomenon when they have to pass through roofs, walls and other conductive objects.

New techniques have therefore been studied by the scientific community, in order to go beyond those limits and allow their usability in a domestic environment.
In the following, the main characteristics an ideal indoor human localization system should have, are analyzed.

- **Reliable, Precise and Accurate:** Considering the rooms of a house as the target environment of use, the accuracy of the positioning system must be much less than the size of the room itself. Moreover, the system must be good in quality and performances, giving always precise information about the position inside the room.

- **Safe and Secure:** The system must not affect the health of people who are localized (safe) and the information about their position or the presence or not of people inside the rooms must be protected and encrypted such that it cannot be used for malicious activities (secure).

- **Easy to use, Passive and Device free:** Considering that the end-user could be an elderly person or without any knowledge of technology, in the ideal case the system should be as easy to use as possible, so that, once installed, the system should operate automatically without the need to perform any specific activities for being localized.
  Many of the best indoor localization systems make use of tags that the user must carry around in order to be located. Although these methods may be simple and inexpensive to implement, especially by exploiting technologies already widespread such as smartphones and smartwatches, they may be, at the end of the day, unreliable because the user could forget to carry the tag with him moving around the rooms of the house. Moreover, the user could be uncomfortable and reluctant to wear a device in every moment of his day, especially in the relaxing moments. For this reason, the passive and tag-less localization systems are considered the most suitable for the scopes of this work.

- **Privacy aware:** The system must be usable and accepted by the user even in environments where, for reasons of privacy, the user does not want to be filmed. For this reason, the acquisition of high-resolution images for human localization should be excluded. In fact, even by ensuring that the captured images would be encrypted, obscured and not used for other purposes, the user would not trust this technology.

- **Unobtrusive:** the system should not interfere with the user daily activities and movements. Furthermore, considering also the surveillance applications, it should be invisible and not easy to be disabled by thieves and intruders.

- **Cheap and easy to install:** Cost plays an essential role in the spread of a product to as many users as possible. It is also important that the system could be easily installed in existing buildings without making difficult and expensive masonry works.

- **Low maintenance and exploitation cost:** A localization system must not require the user to spend a lot of money on maintenance or to keep

the system on. A low power system for long battery life or a wireless power supply system is preferable.

In real life, it is difficult to find a system that is a good compromise among all these specifications. In the next section, some indoor localization systems in the state of art will be analyzed taking care of observe if they present or not the characteristics mentioned above.

1.3 Indoor localization techniques

In this section a brief review of the state-of-the-art methods for locating people in closed environments will be made, analyzing, for each approach, the main features, the advantages and disadvantages [1] [2].

1.3.1 Vision-based method

The use of video cameras for monitoring people inside a room is one of the most traditional methods. Video camera-based monitoring systems are among the most reliable and flexible since they suit a lot of different tasks [3]. In fact, they can be used as an accurate surveillance system, allowing to know exactly and with high resolution what happens in a house while the owners are away, maintain records of the images. It can be used not only to sense the position of the user in a room, but also his movements and gestures, if he is standing or lying on the floor, the activity he is making and his interactions with the environment [4]. Moreover, it can be used to recognize between different users and performing personalized actions according to the case. In spite of all these advantages, it also has several drawbacks that involve energy consumption, cost-inefficiency, an high computational cost and, above all, lack of privacy. In fact, for an application like elderly care and assisted living, monitoring human activities in places such as lavatory and bathroom is necessary since in that places the probability of slipping and getting hurt is high. In these cases the use of video cameras is inappropriate and the user could be contrary to it. Moreover video cameras are ineffective in the dark.

1.3.2 Infrared-based method

Human localization systems based on infrared sensors exploit the human skin's ability to emit infrared radiation. In fact, any objects with temperatures between 0°C and 70°C emit radiation in the long-wavelength infrared

spectrum subsection (from 8 µm to 15 µm). With this method, these particular radiations are sensed and then the processed data are collected in arrays, obtaining a low-resolution image of the indoor environment [5]. Since in indoor environment the human skin temperature is generally higher than the ambient temperatures, from these images it is possible to detect and localize a person in a room. The image collected is actually a matrix that in each cell reports the temperature of a precise spot of the room, so no privacy problems arise with this solution since nothing more than shapes can be distinguished by the acquired data. By using low-resolution infrared sensors the respect for privacy is even higher. The main problem of this kind of solution is the fact that in the home environment there can be another heat source different from human bodies that can radiate at a similar frequency influencing the measurement signal. An example can be a mug of hot chocolate on the table or a radiator. For solving this problem a solution could be to study the heating process of different objects and to adapt the localization algorithm in order to distinguish between a human being and an inanimate object.

More details about the infrared sensor method will be presented in Chapter 2.

1.3.3 Motion-based method

Nowadays every smartphone and smartwatch is equipped with gyroscopes and accelerometers. This kind of sensors can be used in order to detect, starting from a reference point, how far and in which direction the user is going. In fact, the data from the accelerometer can be used to detect each step the user takes and the corresponding step length while gyroscope data can help decide the direction change for each step [6]. This method is very easy and cheap to implement since the user does not need to buy additional hardware, he already has it in his pocket. However physical discomfort issue could raise for the user because he must bring his smart device always with him in order to be localized. Moreover, the intense use of accelerometer and gyroscope lead to a power consumption problem that would drain the phone battery very quickly. Another problem is a linear increasing error that is directly proportional to movement time [7].

1.3.4 Sound-based method

Making use of only microphones, this method localizes a person as a sound source. It is, in fact, possible to deduce the direction of a sound by simply

analyzing the difference in the arrival time of the sound in three or more microphones placed in different spots of the room and interpolating the data using triangulation [8] [9]. Accuracy and reliability of the system can be improved by increasing the number of microphones.

This technique obtains positions and distances of a person with centimetre-scale accuracy in a quite inexpensive and without any annoyance to the user. However the sensing can be easily influenced by other audio signals or noise, so it is prone to false detection.

1.3.5 Ultrasound-based method

Ultrasonic waves belong to the spectrum of sound waves with frequencies so high that are above the human ear's audibility limit of about 20 kilohertz. Using them for localization purposes is not a human invention: many animals, such as bats and cicadas, use ultrasound to locate their prey in hunting. Using ultrasounds for indoor positioning systems makes it possible to achieve a good accuracy of few centimetres due to the slow propagation speed and the low penetration in walls of ultrasound signals [10] [11].

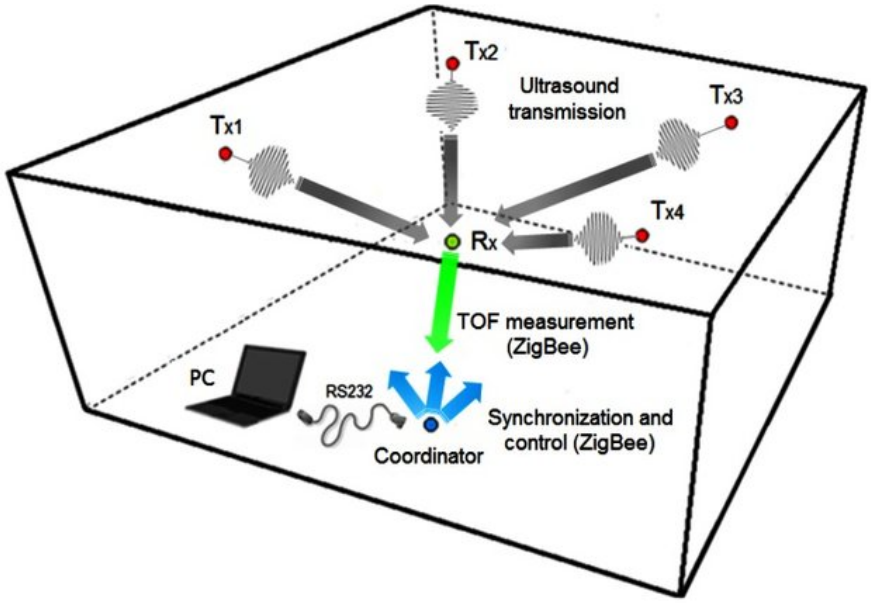

Figure 1.1. Localization with ultrasound sensors system[10]. A set of fixed ultrasonic transmitters are placed on known positions while the mobile node operates as an ultrasonic receiver. A coordinator node is connected to a PC coordinating and managing all other nodes of the network.

The operating principle is based on calculating the distance between receivers and transmitters having known the propagation speed of sound in the transmission medium and the time of departure and arrival of the signal. A correct temporal synchronization of the network nodes is required for a precise calculation. The transmitters nodes are usually placed on the ceiling while individuals need to carry a mobile receiver with them, allowing the line of sight between transmitters and receivers.

An example of how the system is organized is presented in Figure 1.1.

Summing up, despite the high accuracy, reliability and the low cost of infrastructure, the problem of this method is the fact of not being tagless. For its advantages, this method can be used for obtaining some reference measurement in the testing phase of other localization systems. Other details about an application of this method will be given in Section 3.2.

1.3.6 Radio Frequency-based methods

Several localization methods use radio frequencies to localize people in a room. Most of them exploit technologies already widespread in PCs and smartphones for communication purposes such as IEEE 802.11, Bluetooth, Zigbee, RFID and Ultra-Wideband (UWB).

In general, the primary methods used for positioning are [12]:

- Time of Flight (TOF): the position is estimated by calculating the time it takes for electromagnetic waves to travel the distance from a transmitter to a receiver.
- Angle of Arrival (AOA): the angle between an anchor point and the sensor with respect to a coordinate system is measured and from this information, the position is obtained.
- Signal Strength: exploits the fact that the signal from radio transmitter gradually falls off in strength as the receiver moves further away from the receiver.
- Phase: the phase difference between the transmitted and the received signal is used for measuring the distance.

The first wireless network localization systems to be developed required users to carry tags with them. In the last years also device-free RF system has been realized. In fact, many studies about the effects of human presence

on the RF signal strength [13] claim that the human body produces both constructive or destructive interferences in wireless radio network environment, changing the RF communication pattern between the wireless transceivers. This radio irregularity, always considered as a drawback has been exploited to locate the human presence in the indoor environment and even discriminate human activities or gestures [1].

Among all the technique developed, the RSSI method is quite widespread [14]. First, the system must do an offline measurement in order to learn the signal strengths at all locations in the area of interest when there is no human presence. Then, the online real-time measurements are compared with the offline ones in the database to estimate the user location by analyzing the differences in the signals.

The advantages of this method lie in the fact that the infrastructure used is already present in many homes, therefore there are no costs to be added for the purchase and placement of the sensors, just an adequate algorithm to analyze the characteristics of the RF signal is needed. Another positive point is the fact that the fingerprints collected during the offline phase are on average stable over time unless relocation of the Access Point or the introduction of new bulky objects within the area, which normally does not happen often.

However, it requires additional time and work for the user in order to collect the data in the "offline phase". Moreover, other radio devices that transmit at the same frequency of Wi-Fi could interfere with the system and give some faults. An other fact to consider is the safety: authors in [15] claims that repeated Wi-Fi studies show that Wi-Fi causes oxidative stress, sperm/testicular damage, neuropsychiatric effects including EEG changes, apoptosis, cellular DNA damage, endocrine changes, and calcium overload.

1.3.7 Visible Light-based method

In recent years visible light communication (VLC) [16] using light devices such as light emitting diodes (LEDs) has been developed. In [17] it is explained how is it possible to use LED both for illumination and positioning purposes. With this technique, the intensity of the light of the LEDs present on the ceiling is modulated through on-off switching, also known as “on-off keying” (OOK), in order to send a packet of bits. This modulation method is common in VLC and is usually called “intensity modulation” (IM) and is made at a frequency such that the human eye cannot see any modification in the intensity of illumination. Signals from the transmitters (LEDs) are then

received by an optical sensor (a photodiode or a camera) that the human to be localized in the room must wear. The communication takes place through a channel that can be any line-of-sight (LOS) paths from the lights to the receiver. The characteristic of the received signals is then elaborated through some positioning algorithm to obtain information about the position. This architecture is similar to WiFi-based and Bluetooth-based location systems, but using visible light as the carrier does not contribute to the increasing crowding of the electromagnetic spectrum band allocated to Wi-Fi [18].

The main advantage of this technology lies in the fact that it can be easily integrated into a domestic environment by just replacing normal bulbs with special ones suitable for VLC. This would involve a negligible deployment cost. Furthermore, it is a green technology, safe for health and with a long lifetime. The disadvantage lies in the fact that the human to localize must carry a receiver and that must lie in the LOS of the LED. The receiver can be a small and cheap light sensor board connected to the smartphone through the audio port, utilizing Analog-to-Digital Converter (ADC) in the audio to sample the signals. If the VLC technology will have success in the next years probably this receiver will be already integrated into modern smartphones but at this moment this technology is not so widespread, so it would be difficult for the user to find all the necessary equipment.

1.3.8 Pressure-based method

One of the most intuitive and traditional positioning system technology consists in installing some pressure sensors grid on the floor and use the change in pressure resulting from a person passing over it in order to localize it [19]. This method has many positive aspects because once installed under the floor it is invisible, unobtrusive and privacy-aware. Moreover, taking advantage of the differences in weight that may exist between the inhabitants of a house, it can be used for user identification making it possible to distinguish between different users or between an adult and a child or between a human and a pet [20], [21].

The main disadvantage consists in the installation. In fact, it is laborious and expensive and requires sufficient space beneath the floor surface and a flexible flooring on the top of it. Even maintenance work is not easy to carry out because it would be needed to dismantle the floor in order to implement it.

1.3.9 Capacitive-based method

Between people, devices and conductive objects, a natural capacitive coupling is always present. Electrical capacitance is defined as the electrical charge stored on a conductive object divided by the resulting change of its potential. This quantity depends on the size of the conductive object, the distance to other conductive objects, the dielectric properties of the objects and of the dielectric between them (e.g., air).

This physical property is the basis of capacitive sensing, a method that can be used to detect touch, proximity, or deformation. This method has been widely used in the last decade for realizing touchscreens and touchpads on phones, tablets, and laptops but can be also applied in the human indoor localization field. In fact, since the human body is made of conductive material, its distance from a capacitive sensor can be measured in an indirect way by measuring the capacitive coupling between them.

Capacitive sensors consist of sensing electrodes that basically are metallic plates placed on the walls of the room. In general, the sensing can be [22]:

- Active: with this technique a transmitter electrode generates a known signal that is received by a receiver electrode. Both the electrodes are capacitively coupled one onto the other and onto the human body to localize. The difference in the strength of the signal is an indication of the presence and movement of the body.

- Passive: with these techniques, no signals are sent but the existing electric fields are passively sensed by the electrodes. In this way, it is possible to sense human activities with minimal power and infrastructure. However, because of its principle of operation, passive systems tend to be less precise and more susceptible to changes in their environment.

Another distinction can be made considering the operating mode of the capacitive sensing system that relies on the relative position between the transmitter and receiver electrodes and the human body:

- Loading mode: this technique is an active, self-capacitance sensing mode since only one electrode is used both for transmitting and receiving. If a body gets close to the electrode, it loads the electrode causing a displacement current to flow through the body to the ground. This current increases as the distance between the body and the electrode decrease.

- Shunt mode: with this technique, there are two electrodes, a transmitter and a receiver. Since there is a capacitive coupling between the 2

electrodes, a displacement current flowing from the transmitter to the receiver electrode is also present. As the human body approaches the electrodes it causes a capacitive coupling with both the electrodes and a reduction of the displacement current flowing from the transmitter to the receiver electrode. By measuring that current it is possible to obtain the position of the body.

- Transmit mode and Receive mode: the working principle of these techniques is similar to the one used in the shunt mode, what changes is the position of the body with respect to the R/T electrodes. If the body is much closer to the transmitter, it essentially becomes an extension of the transmitter electrode since the coupling between the body and the transmitter is much greater than the other couplings. In this case we are in transmit mode and for obtaining the position of the body is sufficient to measure the increase of the displacement current into the receiver electrode when the body gets closer to it. The inverse of transmit mode is the receive mode.

A drawing of the described modes is in Figure 1.2.

In all these techniques the role of ground is very important: without a common potential, capacitive sensing systems do not have a shared reference and the measurement would be incorrect.

The main advantage of this capacitive sensor method is the fact that it is a tag-less, unobtrusive and privacy-aware technique that, once installed does not need any action from the user in order to do its work. Moreover, since electric fields can propagate through insulators, sensors can be hidden behind some covers and become totally invisible and unobtrusive for the users. These systems are also not expensive because electrodes are usually manufactured from relatively cheap conductive materials (e.g. copper).

A disadvantage can be the fact that the sensitivity of the plate changes with the distance of the body from it, such that it is more accurate in short distances rather than long distances. Moreover the measurement can be influenced by big conductive objects that can be placed in the room such as a fridge or metal shelving.

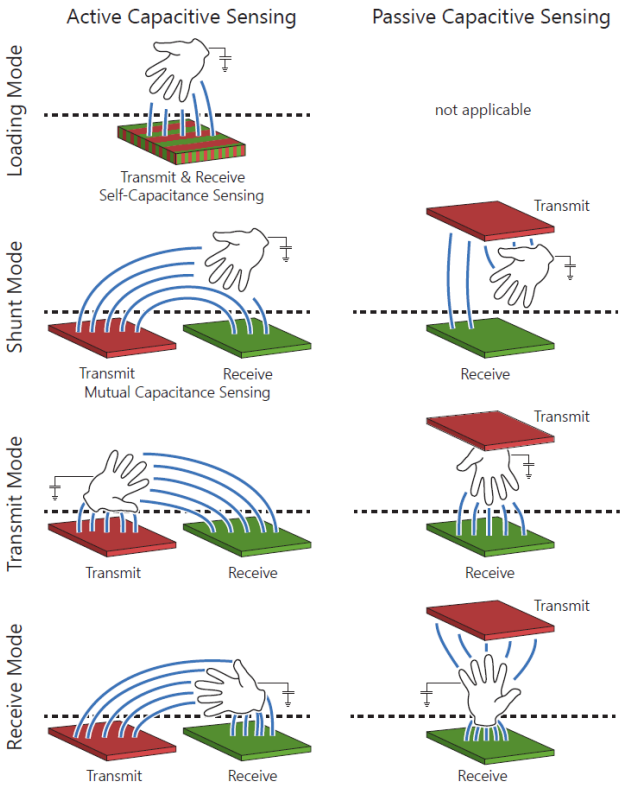

Figure 1.2. Overview of the main capacitive sensing techniques [22].

1.3.10 Summary of the State of Art

In Table 1.1 a summary of the methods described in this section and their main characteristics.

Table 1.1. Comparison between the most used Indoor positioning systems. Data inside the table have been taken by different articles cited in this chapter, but in particular from [1], [2], [14], [17].

Methods	Accuracy	Price	Safety	Tag	Privacy	Power	Notes
Vision-based	high	high	yes	no	no	high	High resolution but lack of privacy and high cost
Infrared Sensors	20 cm	low	yes	no	yes	low	Privacy aware, cheap but hot sources can give faults
Motion	1m	low	yes	yes	yes	high	Easy to implement, costless if you have a smartphone but not tag-less
Sound	33 cm	low	yes	no	yes	low	Cheap but other sources of sound different from the person can interfere
Ultrasound	5 cm	high	yes	yes	yes	medium	High accuracy but not tag-less
RSSI	0.5 m - 3 m	low	no	yes/no	yes	high	Cheap if you have a wifi system already present but not safe and prone of error due to wifi band congestion
VLC (LED)	22 cm	low	yes	yes	yes	low	Cheap, safe, green but the technology is not widespread
Pressure sensor	5 cm	high	yes	no	yes	low	Accurate, unobtrusive but difficoult and expensive to install
Capacitive	15 cm - 30 cm	low	yes	no	yes	low	Tagless, unobtrusive, privacy aware but noisy and sensitivity depends on distance

Among the systems analyzed, Vision-based system could reach the highest accuracy and would give a lot more information about the person to localize w.r.t the other techniques. However, its lack of privacy makes it not suitable for indoor localization purpose. The system that, most of all combine high accuracy and privacy awareness is the ultrasound sensor system that, however, could be difficult to use in a smart home or assisted living environment for the fact that it is not tagless. Talking about costs, the cheapest systems could be the ones that use existing infrastructure or equipment that is already in the pockets of many users. Among that, the motion-based technique, that uses the smartphone to localize, the RSSI that uses the WiFi connection,

present in most of our homes, the sound system based that can exploit the use of every kind of microphone. However the first is not tagless and could be uncomfortable for the user to always bring the smartphone with him. The second could be tagless but it could suffer from interference from other radio devices transmitting at the same frequency and also safety problem due to the constant exposure to radiofrequency could arise. The third method, that is based on sounds the human produce could be full of errors since other sound sources different from the user could interfere. Another cheap localization system is represented by the VLC based method that is a novel and interesting approach to the indoor localization problem, but the technology is not widespread and users could have difficulty in finding the instrumentation needed.

The other systems analyzed need an initial installation phase which can also lead to masonry work, in the worst-case scenario. This is the case of pressure sensors since for installing them it is necessary to remove the floor. Despite the advantages that such a system can have (accurate, unobtrusive), the initial installation cost makes it inaccessible from an economic point of view. The infrared sensor and the capacitive sensor, instead, even if they need an installation phase, no large masonry work is necessary: the capacitive sensors can be attached to the existing walls and covered, to make them invisible, with non-conductive materials, while the infrared sensors simply have to be glued to the ceiling or anywhere in the room. These two systems have not the best accuracy among all the systems analyzed but their accuracy is quite enough for the indoor localization purpose. Moreover, both of them are cheap, safe, tagless, do not consume much power and are privacy-aware.

1.4 Related works

This thesis is part of a larger project a research team at the Department of electronics and telecommunications (DET) of Politecnico di Torino is working on.

The project has the aim of inferring the indoor position and the trajectory of a person using long range capacitive sensors, digital filters, and neural networks.

The front end of the system has been made with a capacitance plate (that acts as transducer) operating in load mode, a relaxation oscillator that converts the measured capacitance into frequency, a micro-controller used for collecting the data and send them over radio using an XBEE module. Once

received, each sensor data is processed using digital filters, then the data labelled with the person position within the room has been used to train and test some machine learning classifiers to infer the location of the person in the room.

In order to achieve an increase in the sensing range, several experiments on the capacitive plates and data processing techniques have been applied.

In particular, in [24] the design, implementation and experimental results of the capacitive sensor node have been presented. Four capacitive sensors, each attached to a wall of a 3 m x 3 m room have been used for the localization of a single person inside the room. Different sizes of plates (4 cm x 4 cm, 8 cm x 8 cm and 16 cm x 16 cm) and several localization algorithms have been tested in terms of precision, recall, average distance error, and detected walking path. Has been observed that all these parameters improve significantly with the increasing of plate area. The 16 cm square sensor plate has been chosen and an ad hoc conditioning circuit has been designed. The details about capacitive-sensor front-end interface design have been presented in [27] and [28].

Since the capacitive sensors have a distance-capacitance dependency that is strongly-nonlinear and degrades the signal-to-noise ratio, advanced processing techniques to improve the sensor performance are required. In [25] the post processing of the data collected from the sensors have been done by exploiting some Machine learning classifiers from the Weka collection. Has been observed that the use of machine learning classifiers can effectively mitigate sensor data variability and noise due to environmental conditions. Comparing the localization performance of different algorithms, its variation with the training set size, and the algorithm resource requirements for both training and inferring, authors have found the best solution algorithm for this scope in the Random Forest algorithm. In [30] all the detail about the architectures used for the neural network and the analysis of the results obtained are summarized.

In Figure 1.3 is shown a schematic of the overall system.

Furthermore the use of capacitive sensors for human identification has been explored. In [26] authors have noticed that human bodies with different BMI have different influences on electric fields at different frequencies concluding that capacitive sensors can successfully distinguish between the people with significantly differeces in weight but that for a more accurate identification a system with more sensor plates is needed. Remaining in the field of human identification, in [29] the electric and dielectric properties of

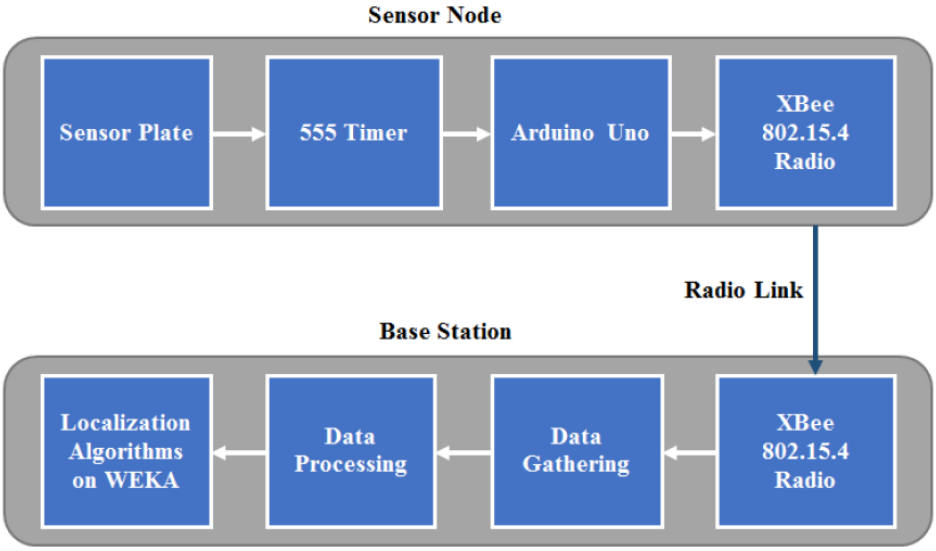

Figure 1.3. Main building blocks of capacitive sensor Node and Base Station. Four sensor Nodes were connected to a single Base Station [25]

human body tissues have been exploited in order to discriminate among different users. Based on the fact that each body has a unique composition, this method represent a refinement with respect to the previous work, improving the sensitivity and discrimination capability of the sensor.

Starting from the indoor localization system presented in this section, this thesis work aims to add to the capacitive sensor network an infrared thermal sensor by exploiting the sensor fusion technique in order to improve its performance, reliability and accuracy. More detail about how the capacitive sensor nodes have been used in this project will be given in Section 3.1.

1.5 Sensor fusion

Sensor fusion is a technique that allows combining data provided by different sensor sources in order to obtain better results compared to what it would have been possible to obtain using the same sources individually. This can lead to obtaining more precise, more complete and more reliable values.

Traditionally, systems have one sensor transmitting information to a single application. This single-sensor measurement method generally suffers from the following problems [23]:

- Sensor deprivation: The breakdown of a sensor element causes a loss of perception of the desired object.
- Limited spatial coverage: An individual sensor usually covers a restricted region.
- Limited temporal coverage: Some sensors need a particular set-up time to perform and to transmit a measurement, thus limiting the maximum frequency of measurements.
- Imprecision: Measurements from individual sensors are limited to the precision of the employed sensing element.
- Uncertainty: From a single sensor the uncertainty is difficult to be reduced since it can depend on missing data (e.g., for occlusions) or ambiguity in the collected data.

These problems can be overcome by using sensor fusion. In fact, by using multiple sensors, either homogeneous or heterogeneous, robustness and reliability are increased by adding redundancy, spatial and temporal coverage are extended and resolution and uncertainty are improved.

In the sensor fusion scenario, different configurations of sensors can be made. In general, they fall into three categories:

- Complementary: the sensors of the system do not directly depend on each other but they can be combined to give a more complete view of the quantity under measurement.
- Competitive: the sensor of the system are independent one from the other and delivers measurements of the same property
- Cooperative: the sensor of the system are independent one from the other but the information provided by them are used to derive information that would not be available from a single sensors.

In the context of indoor positioning, sensor fusion allows combining two or more of the techniques analyzed in the previous section in order to mitigate the defects and limitations of a single technique with the advantages of a second technique, when possible. In this work, a sensor fusion approach will be made by combining the data taken independently from a capacitive sensors network and an infrared sensor, in a complementary way.

1.6 Main contribution of this thesis

This thesis work has the purpose of improving the performance, reliability and accuracy of the existing capacitive sensors network localization system described in Section 1.4 by implementing a complementary sensor fusion technique with an infrared thermal sensor localization system designed for this scope. The goal is to obtain a low cost, easy to use, unobtrusive, passive, tag-less and privacy-aware indoor localization system that can be safely and easily installed in smart homes and assisted living environments.

The main problem of capacitive sensors lies in the fact that they have a sensitivity that steeply decreases with the increase of the distance from them. By placing the capacitive sensors on the four walls of a room, the area of greatest sensitivity is represented by the edges of the room itself, while data acquired in the centre of the room are the most afflicted by noise and errors. Placing an infrared sensor in the centre of the room on the ceiling gives additional sensing data in the part of the room where data were less accurate and improving the reliability. Moreover, using two different systems that extract the localization information from two completely different physical quantities, the obtained system would be more robust since the noises that affect one of the two systems do not affect the other and vice versa.

In particular, the present work is so organized:

- The importance of indoor human localization has been highlighted, underlining the characteristic an ideal indoor localization system should have. A review on the state-of-art techniques for indoor localization has been made analyzing for each method advantages and disadvantages (Chapter 1).
- An infrared sensor acquisition system has been designed using an infrared sensor, in particular the D6T-44L-06 MEMS Thermal Sensors, and Arduino board to acquire data about the position of the user. The data acquired has been sent via radio through an Xbee module to a computer where the elaboration and packing of the acquired information have been made with MATLAB (Chapter 2).
- A complete experiment has been set up using four capacitive sensors, the infrared sensor and an ultrasound sensor as reference. The operation of each part has been tested separately (Chapter 3).
- Finally, experimental data from all the sensors have been collected simultaneously in four different experiments. The obtained results have

been analyzed and filtered and merged (Chapter 4).

- Conclusions and observations on possible future developments have been drawn (Chapter 5).

Chapter 2

Thermal Infrared Sensor acquisition System

2.1 Infrared sensor selection

With the prospect of using a sensor fusion technique with the capacitive sensor system, an infrared sensor has been chosen for many reasons. First of all, it is affected by kinds of noise that are often complementary to the ones of capacitive sensors. Moreover, it is a tag-less, not expensive, privacy-aware and safe localization system that can be easily placed in the target environments (smart homes and assisted living environment).

In the field of infrared radiation sensor, two main kinds of sensors exist:

1. Quantum well infrared photo-detector (QWIP) technology: it is a technique that uses the photoelectric effect for detecting the long-wavelength infrared (i.e., 8–12 µm) radiations. Its principle of operation is based on the inter-band transition of electrons across the band gap (Eg) from the valence band to the conduction band when photons with energy hv $>$ Eg excite it. These photo-excited electrons create a current that is proportional to the number of photons collected and that can be easily measured [31]. This method is really sensitive and has a short response time but it is necessary to cool the photo-detector to a temperature of 70K in order to perform well, which makes it not suitable for the intended application of this project.

2. Thermal detectors: are based on temperature increase in some materials from absorption of IR radiation, which can cause changes in the material characteristics. Among the advantages, their detectability is nearly

wavelength-independent (flat spectral response), they do not need a cooling operation and they usually work at room temperature and has a lower cost, compared to quantum detectors. Disadvantages include lower sensitivity or detectivity and slower response speed (normally in milliseconds) [32]. Today, the most common thermal detectors are:

- Microbolometer: is based on the temperature-dependence of an electrical resistance whose value changes when heat radiation is absorbed. The change in resistance causes a change in the signal voltage drop across the bolometer resistance that can be easily measured. In order to achieve high sensitivity and large specific detectivity, it is necessary to use a material with a high coefficient of the temperature of electrical resistance. A drawback is that this method is quite expensive and an initial temperature stabilization is necessary before the use.
- Pyroelectric sensors: also called Passive InfraRed (PIR), they are made with materials that generate energy when exposed to heat (pyroelectric materials). PIR does not autonomously detect movement but it detects sudden changes in temperature which modify the state that the PIR had previously memorized. When someone passes in front of it, a rapid change in the detected temperature is caused and the person is located. The movement of objects of identical temperature with respect to the background, of course, is not detected. In [34], authors use a set of PIRs to implement a human movement detecting system that is able to recognize the direction of movement, the distance of the body from the PIR sensors, the speed of movement during two-way, back-and-forth walking and identify the walking subject. This kind of system cannot be used for human localization purposes since the PIR sensors can only detect changes in heat flow and would not detect the presence of a person steady that does not move.
- Thermopiles: it is composed of several thermocouples connected in series that exploit the Seebeck effect in order to detect the temperature of the object under observation. In other words, they are stacks of junctions of two different material [33] that are called active and passive junctions.

  As can be seen in Figure 2.1 the active junctions are attached to a thermally isolated membrane that is exposed to radiation, while the passive ones are only influenced by the ambient temperature. A

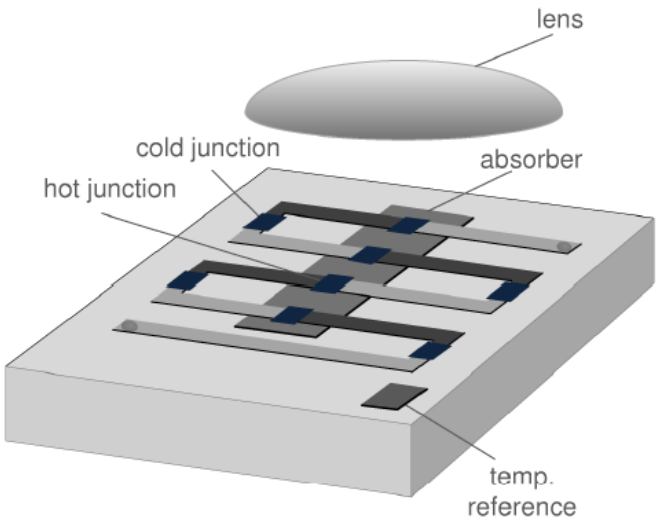

Figure 2.1. Structure of a thermopile [5]

voltage difference proportional to the temperature difference at the junction is then created. In this way, it is possible to measure the effective temperature of the object.

The response times of this technology is usually between 20 ms and 50 ms, so they are fast enough for the detection of human motion.

Summing up, for thermal human indoor localization the best solution is to use thermopiles because:

1. unlike pyroelectric sensors, their output does not depend on the rate of change of the object's temperature;
2. unlike bolometer-based devices, thermopiles do not require special temperature stabilization and they are cheap;
3. unlike quantum based technique they do not necessarily need cooling.

For all these reasons, thermopiles technology has been chosen for this work.

2.2 Omron D6T MEMS Thermal Sensor

The sensor chosen for this work is the D6T-44L-06 MEMS Thermal Sensor by Omron [35], [36], [37]. This component uses the thermopile technique to

give information about the surface temperature of an object in arrays of 16 pixels (4x4). The main characteristics of this sensor are reported in Table 2.1. As is can be seen it has a maximum object temperature output accuracy of ±1.5°C. Talking about resolution, it can be expressed in terms of "Noise Equivalent Temperature Difference" that is a measure for how well a thermal imaging detector can distinguish between very small differences in thermal radiation in the image. For this sensor, the value is equal to 0.14°C.

Table 2.1. Overview of the characteristics of Omron D6T MEMS Thermal Sensor

Item	Power supply voltage	View angle	Temperature accuracy	Temperature resolution (NETD)	Current consumption
D6T-44L-06	4.5 to 5.5 VDC	X direction: 44.2° Y direction: 45.7°	±1.5°C max (VCC= 5.0 V, Ta= 25°C)	0.14°C	5 mA (typical)

In the following sections, some other details about this infrared thermal sensor and the design choices will be discussed.

2.2.1 Operating principle

The inside of a D6T MEMS Thermal Sensor is shown in Figure 2.2. As it is possible to see from the image, a silicon lens on the top of the sensor is present in order to collect the far-infrared rays emitted by an object onto the thermopile sensor present in the module. These infrared rays arrive in the thermopile sensor inside and an electromotive force is then created. A specialized downstream processing circuit adjacent to the sensor chip is present in order to achieve low-noise temperature measurements.

An analog circuit inside the module converts the electromotive force generated by the thermopile in temperature information, obtaining both the temperature of the object and the temperature value inside the module. Finally, the measured value is converted to digital information and outputted through an I2C bus.

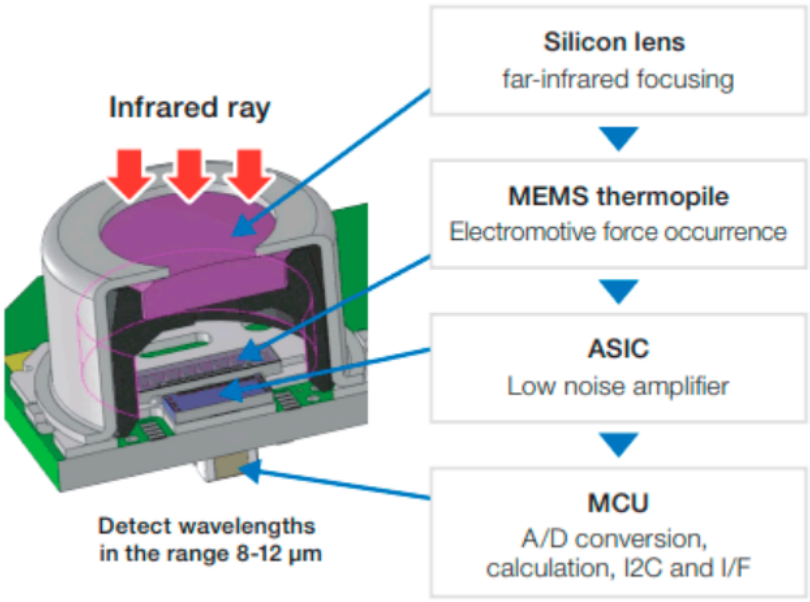

Figure 2.2. Inside detail of D6T MEMS Thermal Sensor [35]

2.2.2 Field of view

On the top of the thermopile sensor, the silicon lens present in the D6T module is optically designed in order to extend the sensitivity characteristic view angle of the sensor. In order to calculate the actual area where the sensor can detect the presence of a human, the Field of View indication must be taken into account. The user manual defines the Field of View of the sensor as an area angle of 50% for maximum sensitivity. As can be seen from Figure 2.3 the Field of View in the X direction is equal to 44.2° while in Y direction is equal to 45.7°.

From these value it is possible to measure, by applying simple geometric equations, the total measurable area (FOV) of the sensor, that, of course, enlarges as the distance between the measured object increases. For example, when placing the sensor at a height of 1 meter from the floor, it will cover an area of 81 cm x 84 cm on the wall while if it is placed at a distance of 3 meters from the floor, the covered area will be 244 cm x 253 cm that is much larger (as can be seen in Figure 2.4). However, as the distance increases, the occupancy ratio of objects (people) in the FOV reduces and the measured

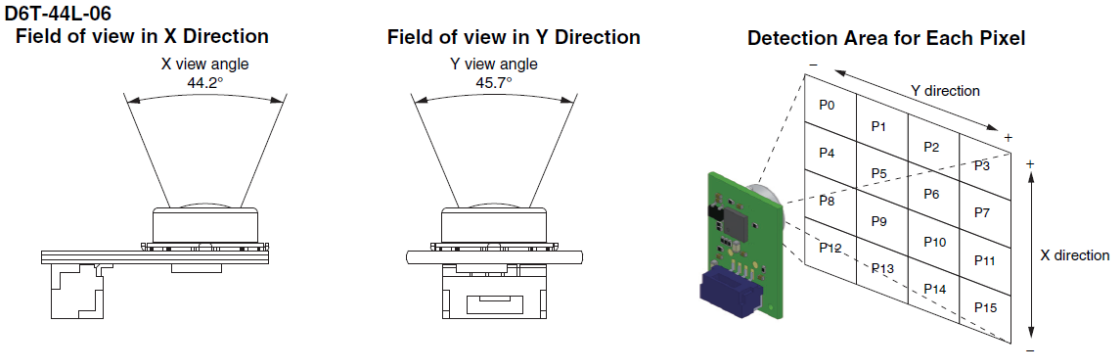

Figure 2.3. Angle of view of D6T-44L-06 MEMS Thermal Sensor by Omron [35]

temperature values are strongly influenced by the background temperature than the temperature of the intended object (people).

In conclusion, to correctly detect the presence of a person using this sensor, the measured object must not be too small with respect to the total FOV area since it is designed only for close-distance applications.

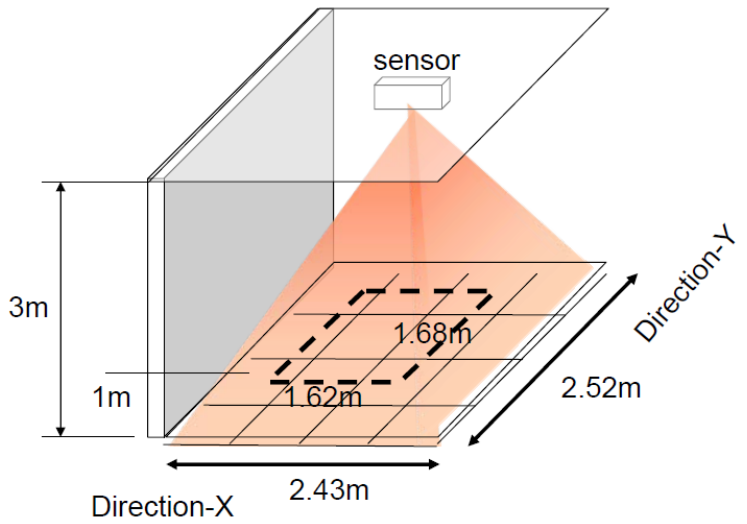

Figure 2.4. Field of view area positioning D6T sensor at 3 m and at 1 m from the floor [37]

2.2.3 Transmission of data through I2C

The I2C communication protocol is exploited by the D6T-44L-06 MEMS Thermal Sensor for the communication of the sensed temperature data array. This hardware protocol requires two serial communication lines: SDA (Serial DAta) for data and SCL (Serial CLock) for the clock. Together with these 2 wires, a reference connection and a power supply line are also present (Figure 2.5). Both SDA and SCL are bidirectional lines, connected to a positive supply voltage via pull-up resistors.

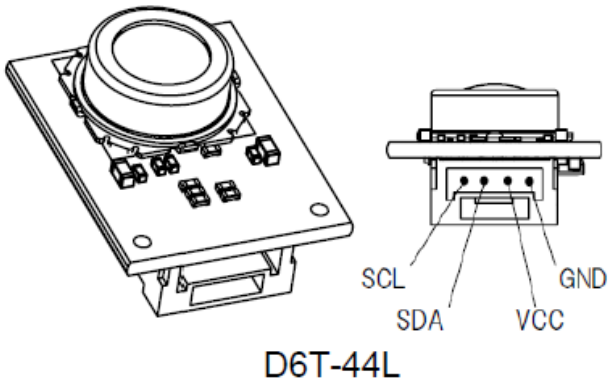

Figure 2.5. Outer view and connections of the Omron D6T-44L-06 MEMS Thermal Sensor [36]

The protocol is based on a master-slave mechanism in which the master is in charge of initiating the data transfer on the bus and generating the clock signals to permit that transfer. Any other device connected to the bus is then considered a slave and is addressable by a unique address [38].

In the case of the D6T-44L-06 MEMS Thermal Sensor, it acts as an I2C slave. A schematic of the data transfer from the sensor to the master is represented in Figure 2.6. In order to read the data acquired from the sensor is then necessary to connect a microcontroller to the bus, acting as a master, and then to follow these steps:

1. The master must send a start condition that corresponds to a HIGH to LOW transition on the SDA line while SCL is HIGH.

2. The master sends the clock in the SCL line while is sending the 7 bits address of the slave in the SDA line. In this case, the manual of the D6T states that the address of the sensor is "0001010" in binary. At the end

I2C port condition setting

Device Address	7bit : 0001_010b
	8bit (with R/W bit) Read : 15h , Write : 14h
Data bit width	8bit (MSB-first)
Clock Frequency	max 100kHz
Control for Clock-stretching	On (Auto waiting)

Port-data chart

Case 16ch (D6T-44L)

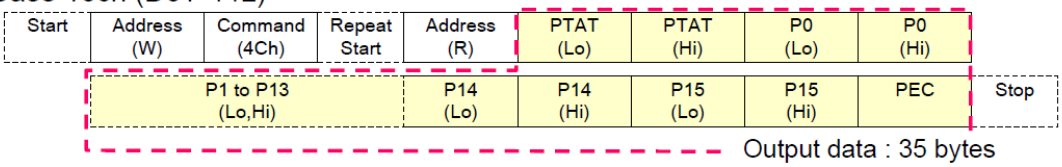

Figure 2.6. I2C data line flow and Output data composition from the datasheet of D6T-44L-06 MEMS Thermal Sensor [36]

of this address word, an eighth bit indicates if the master wants to read (bit at "1") or write (bit at "0") in the slave register. In this case, it puts the last bit at 0 and sends in the SDA line the command word "4C" in hexadecimal. In this way, the slave understands that it will be requested to send the acquired data.

3. A repeat start condition is then sent by the master followed by the address of the slave and, this time, a Read request.

4. If the addressed slave has received the command it takes control of the data line on the next high pulse of the SCL and it forces the line to be low (acknowledge condition). In this way, the master will be sure that the slave is ready to send the data.

5. The slave sends the data to the master in groups of 8 bit. As is can be seen in the bottom part of Figure 2.6, the total packet of output data is composed by 35 bytes and includes the reference temperature inside the sensor module (PTAT), the array of 16 temperatures read by the sensor(from P0 to P15), and a byte for the cyclic redundancy check (PEC).

6. At the end of the transmission, the master declares the end of the transmission by sending a STOP condition that corresponds to a LOW to HIGH transition on the SDA line while SCL is HIGH.

In Figure 2.7 two images of SDA and SCL signal taken with the oscilloscope during a data transmission of the D6T sensor are presented. In particular, on the left, a start condition is shown while on the right a stop condition is present.

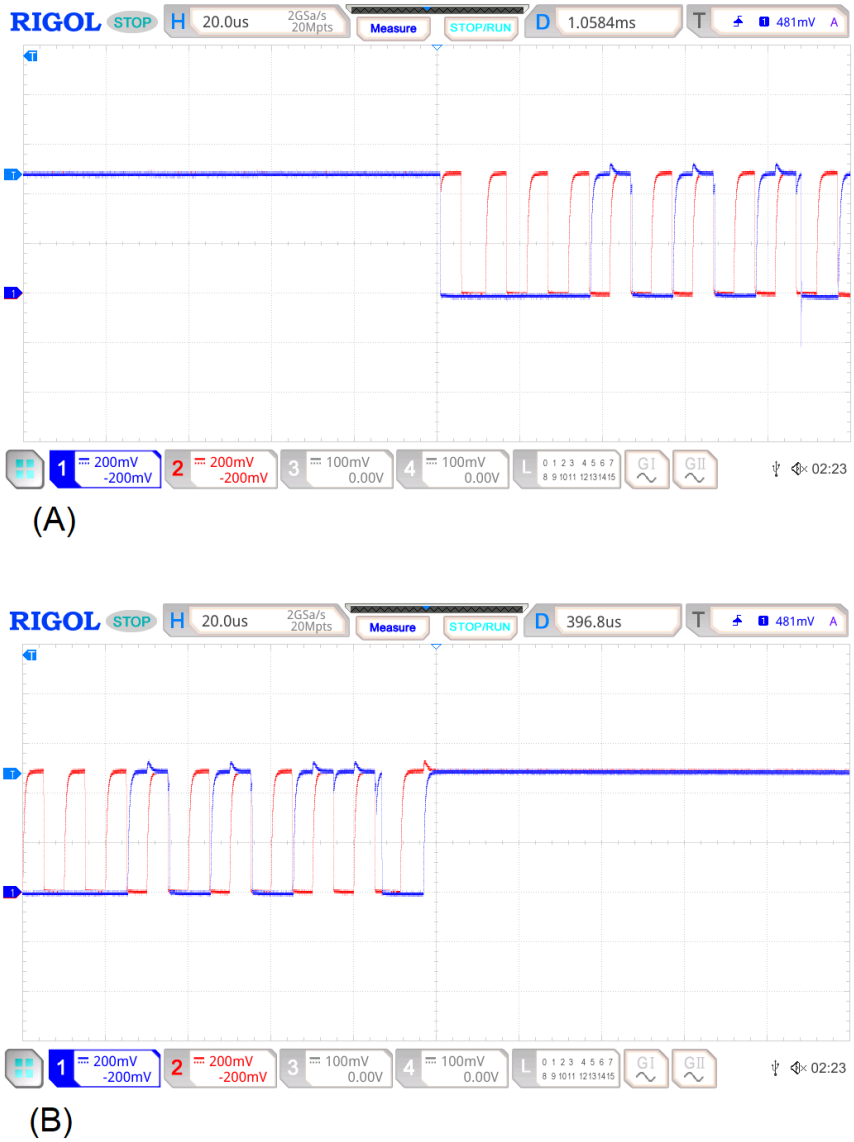

Figure 2.7. Start and Stop of a transmission from D6T sensor to the master using I2C protocol. Red lines represent the SCL signal while blue lines represent the SDA signal.

2.3 System implementation using microcontroller

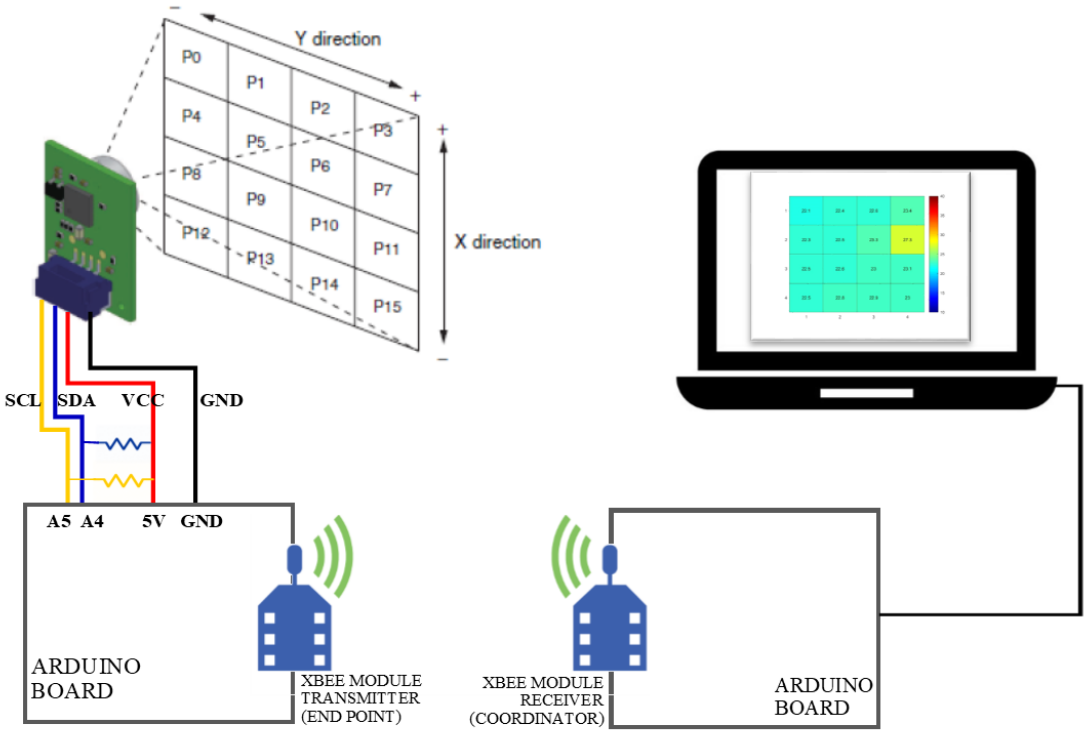

Figure 2.8. Schematic of the overall infrared thermal system. Image realized based on [35]

The acquisition of data from the sensor has been done using the microcontroller of an Arduino Uno board. Arduino Uno is a microcontroller board based on the ATmega328P, a CMOS 8-bit microcontroller [39].

In Figure 2.8 the schematic of the overall system. As it can be seen, the sensor communicates the data through a bus using the I2C protocol to the Arduino Uno board which, in turn, sends the collected data via radio to a second Arduino board. The data received are then transferred to a PC via a USB cable and processed using the MATLAB software. In the next subsections all the details about the electrical connection and design choices adopted will be given.

2.3.1 Connection with the Thermal Infrared Sensor

In Figure 2.9 the schematic of electrical connection adopted in order to connect the sensor to the microcontroller.

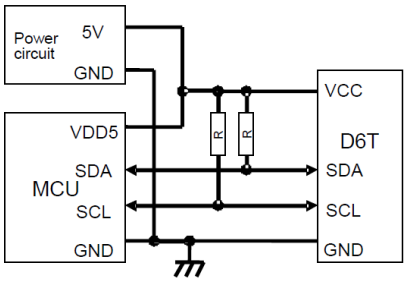

Figure 2.9. Electrical connection between D6T sensor and MCU [36]

Referring to the guidelines of the I2C protocol, a pull-up resistance of the value between 3 kΩ and 10 kΩ has been connected between the two serial communication lines SDA and SCL and the power supply VCC line. The aim of this resistor is to maintain the SDA and SCL lines at a HIGH level when the bus is free and ensure that the signals are pulled up from a LOW to a HIGH level within the required rise time. Several tests were carried out to choose a value that could be fine for this application. In fact, by choosing a pull-up resistance value too close to the upper limit and observing the SCL signal, it is possible to see that the rising and falling time of the generated square wave are longer than the ones observed when a lower value of pull-up resistance is chosen. On the other hand, choosing a too small pull up resistor would give a smaller rising and falling time but higher power consumption and a sharper square wave that would give worst cross-talk effects in the near wires. For these reasons, after some tries, an intermediate value of $6.8k\Omega \pm 1\%$ for the resistor has been chosen.

2.3.2 Wireless communication using Xbee module

Due to the position in which the sensor should be placed, i.e. the ceiling of a room, it has been decided to send the collected data from the sensor via radio to another Arduino board in order to save and elaborate the data in a computer. For this scope, a couple of Xbee modules have been used connecting them to the two Arduino boards using an Xbee shield, as shown in Figure 2.10.

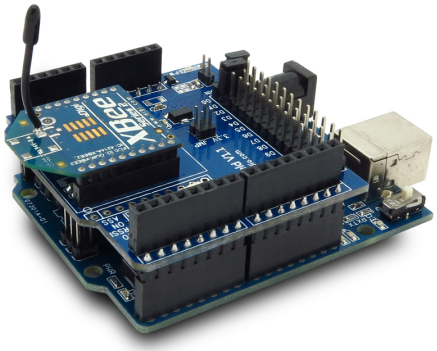

Figure 2.10. Arduino connection to Xbee module through a shield

The Xbee module used is the Digi XBee® Embedded ZigBee modules [40]. It allows making a wireless end-point connectivity between two or more devices using the IEEE 802.15.4 networking protocol. The platform XBee Configuration and Test Utility (XCTU) has been used for the configure and test the Digi RF devices [41]. With this tool has been possible to configure the two modules such that one can act as a coordinator and the other as an end device.

In particular, two unique addresses have been assigned to the two modules and the interface data rate has been set to 9600 bps. A channel of communication different from the one used for the Xbee communication of the capacitive sensors has been assigned in order to avoid interference.

2.4 Programming the Microcontroller using Arduino

The Arduino Software (IDE) has been used to write the programs and upload them to the Arduino Uno boards. In Appendix A the Arduino codes for the acquisition of data and the complete communication are present.

In order to handle the D6T-44L-06 thermal sensor the Wire and WireExt libraries have been used. They define some classes of function that help in the

I2C communication with the sensor, following the rules explained in Section 2.2.3. In particular the start condition with the address of the sensor device is sent followed by the command of starting the communication. Then a repeated start condition is sent to the sensor with a read command. The Data read from the sensor are then saved byte by byte in a buffer until the end of the transmission.

2.4.1 Error detection using CRC and retransmission

At the end of the reception a check on the integrity of the received data is made using the CRC-8 (Cyclic Redundancy Check). In fact the sensor, together with the data, sends also a PEC (packet error code) byte that is appended at the end of each transaction. The CRC principle consists in treating binary sequences as binary polynomials, i.e. polynomials whose coefficients correspond to the binary sequence. In this case the PEC is calculated by the sensor using the following Generator Polynomial G (n + 1 bit) of order 8:

$$C(x) = x^8 + x^2 + x + 1$$

that corresponds to the binary number 100000111. Assumed that this polynomial is known by both the transmitter and the receiver, and being the message (M) to be transmitted any sequence of bits, the CRC will be given by the division of: M/G. For making this division bit-wise XOR and left shift of the bits are used, as represented in Figure 2.11.

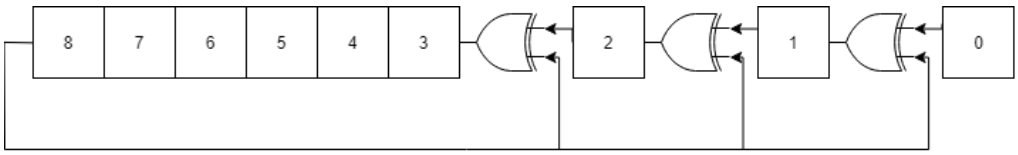

Figure 2.11. Graphical rapresentation of CRC-8

The receiver of the message, in this case the Arduino board, by applying a bit-wise algorithm that mimics the hardware shift register method, is able to compute the packet error code from the received data. The function, defined into the code, that implements the CRC algorithm is reported in Figure 2.12 and is called "calc_crc".

As it can be seen, it receives a byte data that is shifted left of one bit at a time and then, if the MSB is at 1, the division is performed by making a

```
//------------------------------crc calculation function-------------------------
unsigned char calc_crc(unsigned char data)
{int index;
 unsigned char temp;
    for(index=0;index<8;index++)
    {
        temp= data;
        data <<= 1;
            if(temp & 0x80)
            {
                data ^= 0x07;
            }
    }
 return data;
}
```

Figure 2.12. Function implementing CRC-8 algorithm

bit-wise XOR with the number "00000111" in binary (that corresponds to 7 in decimal).

The call of the calc_crc function inside the code in Figure 2.13.

```
// ------------------------crc calculation------------------------


crc= calc_crc(0x15);
for (i = 0; i < 34; i++)
{
  crc=calc_crc(rbuf[i] ^ crc);

}
  tPEC= rbuf[34];


// ------------------------------------------------------------------
```

Figure 2.13. Call of the calc_crc function implementing CRC-8 algorithm inside the main code

As it can be observed, all the 34 bytes received from the sensor are used as input of the function one after the other, making a bit-wise XOR with the previous computed CRC output before sending them to the function.

The resulting byte is then compared to the PEC received at the end of the

transmission with the sensor and in case of inequality, a transmission error is discovered and the sensor is requested to send the packet again. In particular, a design choice of repeating the reading for a maximum of 3 times has been made, in order to not slow down too much the system. A "valid byte" is set to 1 if the transmission has been successful. This check improves the reliability of the bus.

2.4.2 Radio transmission of data through Xbee module

For the sending of data via Xbee the library XBee.h has been used. For the transmitter, in the code a packet of data has been composed using the function Tx16Request() as showed in the Figure 2.14.

```
/*---------------------------------*/
//  bytes to be transmitted
uint8_t payload[33] ;
/*to turn off TX_STATUE _RESPONSE*/
uint8_t frameId = NO_RESPONSE_FRAME_ID;
uint8_t option = DISABLE_ACK_OPTION;
Tx16Request tx = Tx16Request(0xDCBA, option, payload, sizeof(payload), frameId);

/*---------------------------------*/
```

Figure 2.14. Initialization of the packet of data to be sent via radio using Xbee.

In particular, the packet is composed by the address of the coordinator (that is the receiver), the data to be sent, the size of the data sent and some transmission options such as the handling of the acknowledge. Then, using the function "xbee.send()" the packet is transmitted.

From the receiver side, the Arduino board has been programmed with the code present in Appendix A.2. When the data are received an error check is made. If no errors in the transmission are present, the data are saved, unpacked and transmitted to the computer using the serial port.

2.4.3 Sensor data acquisition period

The Arduino code presented in the previous section repeats itself continuously in a loop while the system is running. However, the D6T thermal infrared sensor needs some time to acquire samples, pack and send them to the board. Has been observed experimentally that at least 80ms are required by the sensor for making an acquisition and sending of data. This interval of

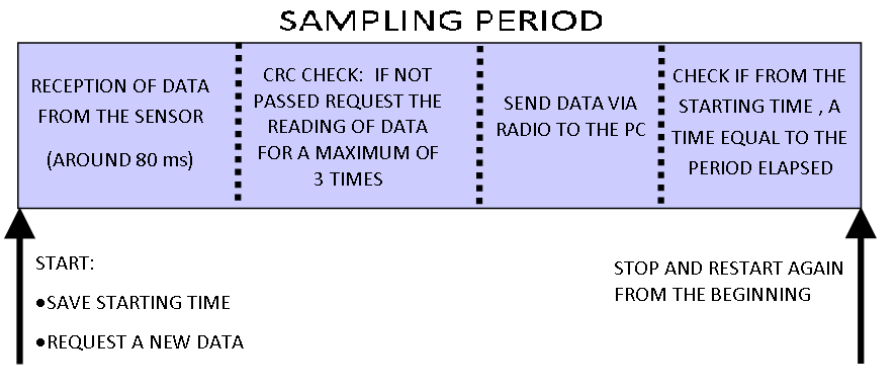

Figure 2.15. Schematic of how the sampling period is organized.

time is not constant and considering that, if an error occurs, the sensor must resend data again, it could be longer. It has been observed that by letting the Arduino continuously ask for data without a pause the communication between the board and the sensor is worst and frequently a communication timeout occurs due to communication mistakes. This timeout condition is implemented with low input on SDA or SCL terminal for one second and should be avoided since for one second the sensor cannot communicate its readings to the board and samples for that period are lost. For this reason, at the end of the code, a timer is set in order to pause the system for the time necessary to complete the period, making a subtraction between period and the elapsed time. In this way, data are received with a fixed sampling rate. In Figure 2.15 the drawing represents a schematic of how the sampling period is organized.

After some observation of the maximum acquisition time, made directly on the signals with the oscilloscope and through software with timestamps, the minimum sampling period has been set to 125 ms, obtaining a rate of 8 samples/s.

2.4.4 Data acquisition with MATLAB

Data received in the computer through the USB serial port have been acquired using the software MATLAB. In this environment it is easier, w.r.t. Arduino software, to elaborate the data saving them in a matrix and then creating spreadsheets and appropriate graphs.

In Appendix B.1 the code used for the acquisition of data in MATLAB

is shown. In particular the code is set to run for a defined amount of time exploiting the "tic" and "toc" functions and a while loop. Data from the serial port COM5 are saved into an array using a fscanf() function. The timestamp of the arrival time of each packet of data is simultaneously saved in an array with a resolution of one millisecond. This operation has been done in order to have a time reference useful for later synchronizing data arriving from the infrared sensor with those from the capacitive sensors.

A spreadsheet file in Comma Separated Values (CSV) format containing the temperature data, the timestamps and the valid bytes are then created.

In order to have a graphical representation of the so acquired data, a heat-map graph from each packet of data is then created using the code reported in Appendix B.2. In this graph, the temperature of each of the 16 squares in which is divided the field of view of the sensor is represented with a colour that has a warmer tone as higher is the perceived temperature. In Figure 2.16 two examples of the output file acquired without and with the presence of a person in the room. It can be seen that the square occupied by the person (i.e. the square with coordinates (4, 2) in Figure 2.16 B) has a higher temperature shown by a warmer colour.

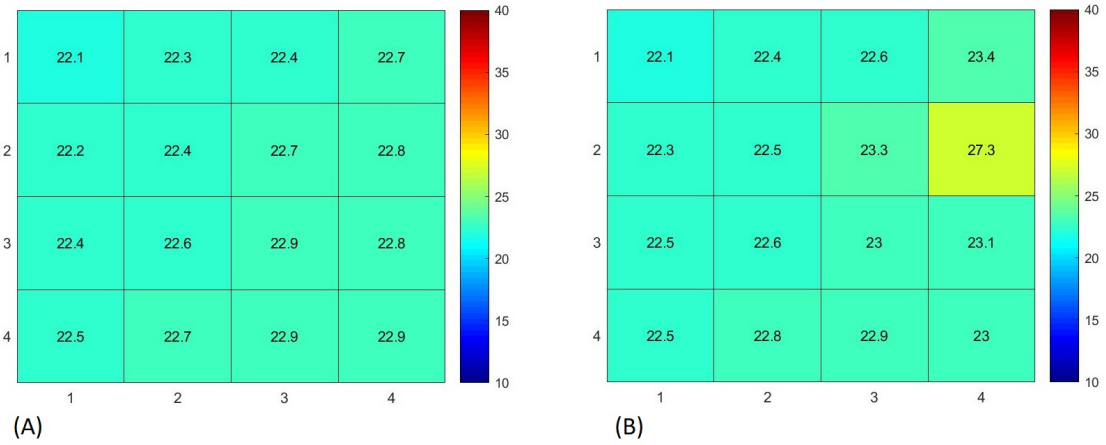

Figure 2.16. Output scheme of the infrared sensor acquisition system. In figure A the image from above of the empty room; in Figure B the presence of a person is highlighted by a pixel with higher temperature w.r.t. the background, shown with a warmer color.

Chapter 3

Experiment setup

The complete indoor localization system includes the thermal infrared sensor system described in Chapter 2 and the capacitive system designed in [30]. In addition to this system an ultrasound sensor network has been installed in order to have an accurate reference for the position of the person in the room.

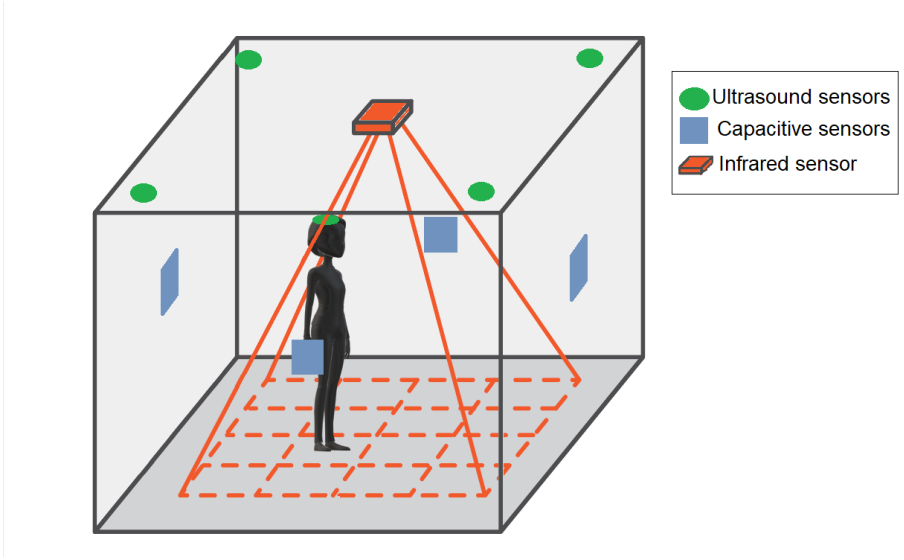

Figure 3.1. Representation of the overall experiment setup

In Figure 3.1 a drawing representing the overall experiment setup. The room used for the experiment is a 3 m x 3 m room with a ceiling at a height of 3.05 m. In this structure, the capacitive sensor plates are placed at the centre of the walls at a height of 120 cm from the floor, the infrared sensor

is placed at the central point of the ceiling and the ultrasound sensors are placed at the four edges of the ceiling and communicate with a tag on the head of the person.

3.1 Capacitive Sensors System

In this section more details about the capacitive sensor indoor localization system used for the experiment will be given. Moreover, it will be explained how the capacitive sensor nodes have been tested and some attempt to improve the sensitivity of the sensors before making the overall experiment.

3.1.1 Capacitive sensor module

The capacitive sensor module is based on a 16 cm x 16 cm metal plate installed at a height of 120 cm from the ground, considering this as an average height of a person's bust. Defining as d the distance between the plate and the human body, plate capacitance cannot be determined analytically for d much longer than the plate diagonal. The measure of capacitance is then indirectly obtained using a relaxation oscillator based on a 555 timer integrated circuit (IC). The timer is configured in astable multivibrator configuration and the schematic of the circuit can be seen in Figure 3.2.

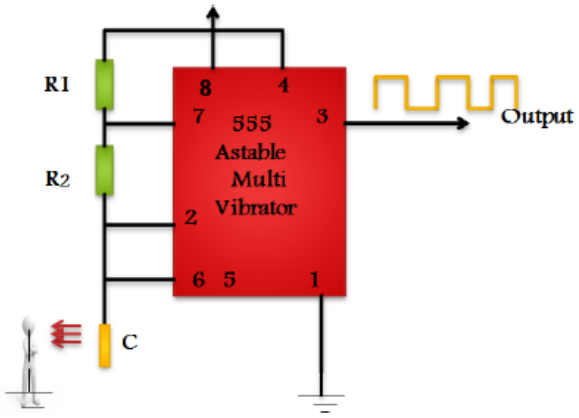

Figure 3.2. 555-based capacitance-frequency converter [24].

The oscillation frequency f of the timer can be represented by the following formula where $R1$, $R2$ are the values of resistors in the multivibrator circuit

and C is the capacitance of the plate:

$$f = \frac{1}{0.7(R1 + 2R2)C} \tag{3.1}$$

As it can be seen, f is inversely proportional to sensor plate capacitance C through a constant determined by the resistor values. From this value of frequency, the distance d of the person from the plate could be then empirically computed.

The frequency information is then collected by a micro-controller that sends it to the base station using a Zigbee radio module. The sensor is battery-powered and has no galvanic connection to the ground.

3.1.2 Testing the module and implemented optimization

Each of the four capacitive sensor nodes has been tested separately in order to check if there was space for improvement. In particular a sensitivity test has been made by moving in front of each sensor in a straight line, starting from a distance of 1.8 meters and approaching each time by a small step of 30 centimeters. For each step 50 samples have been taken with a sampling rate of 5 samples per second.

The sensitivity test has been repeated two times, changing two different kind of timer based on different technologies:

- LMC 555CN by Texas Instument that is based on CMOS logic [43].
- NE 555N by ST-Microelectronics that is based on Transistor-transistor logic (TTL) [44].

In the following graphs in Figure 3.3 it is possible to observe the sensitivity test acquisitions made with the two different 555 ICs at the distances from the sensors: 180 cm, 150 cm, 120 cm, 90 cm, 60 cm and back to 180 cm. The data have been normalized in order to obtain value that could be compared. The average of points at "long range" distance of 1.8 m have been computed and then all points have been divided by this average.

Also the drift has been observed, by acquiring 6000 samples in a 20 minutes reading (5 samples per second), while the room was empty. The normalized plots can be observed in Figure 3.4.

As can be seen, using the TTL based timer (NE 555) a lower noise, yet lower sensitivity are present than using CMOS based (LMC 555). Since noise

can be removed by filtering the data, the CMOS based timer has been chosen after this experiment.

From this sensitivity test has been observed that not all the sensors have the same sensitivity. In particular, sensor 4 seems less susceptible to changes in the capacity of the plate and is able to detect the presence of a person and to locate it at a lower maximum distance compared with the other nodes. This can be due to the position of sensors in the room or to the hardware of the sensor node.

In order to check if the position where the sensor is in the moment of the acquisition could influence the reading, all the measurements have been repeated by placing all the sensors in the same position. No significant changes have been observed with this change of position. For this reason, the HW reasons why the system was not working as good as possible have been analyzed. In particular, all the contacts have been checked with a multimeter, most of the contacts of the circuit board have been re-soldered, the position of the battery with respect to the plate has been changed since it could give some noise. The plate has been also cleaned and the LMC 555 IC has been substituted with a brand new one of the same type.

All these operations have been repeated for all sensors in the same way, but significant improvements have only been observed for two, in particular, sensor 1 and 3, whose graphs of before and after are present in Figure 3.5. As it is possible to observe, an increment of the sensitivity for sensor 1 and a reduction of high-frequency noise have been obtained. For the other two sensors, no significant changes have been observed.

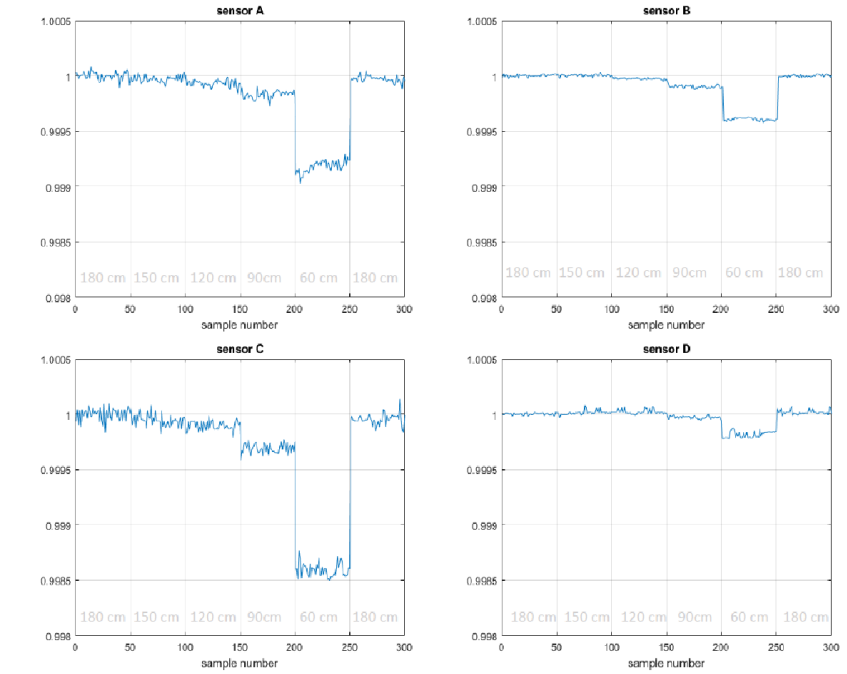

A) Using LMC 555CN

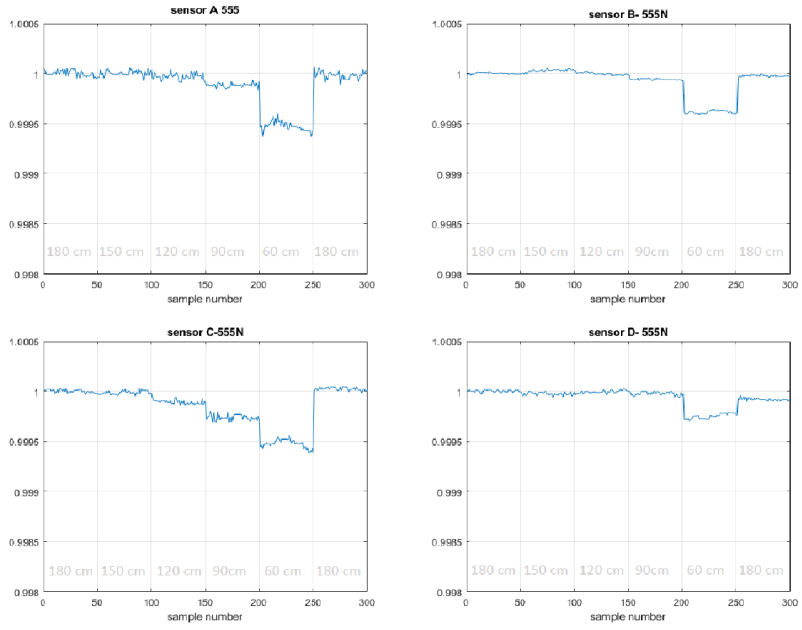

B) Using NE 555N

Figure 3.3. Sensitivity test results made for all the four capacitive sensor nodes and repeated by changing the timer IC. In the upper part (A) data acquired using LMC 555CN by Texas Instruments, in the bottom part (B) data acquired using NE 555N by ST-Microelectronics

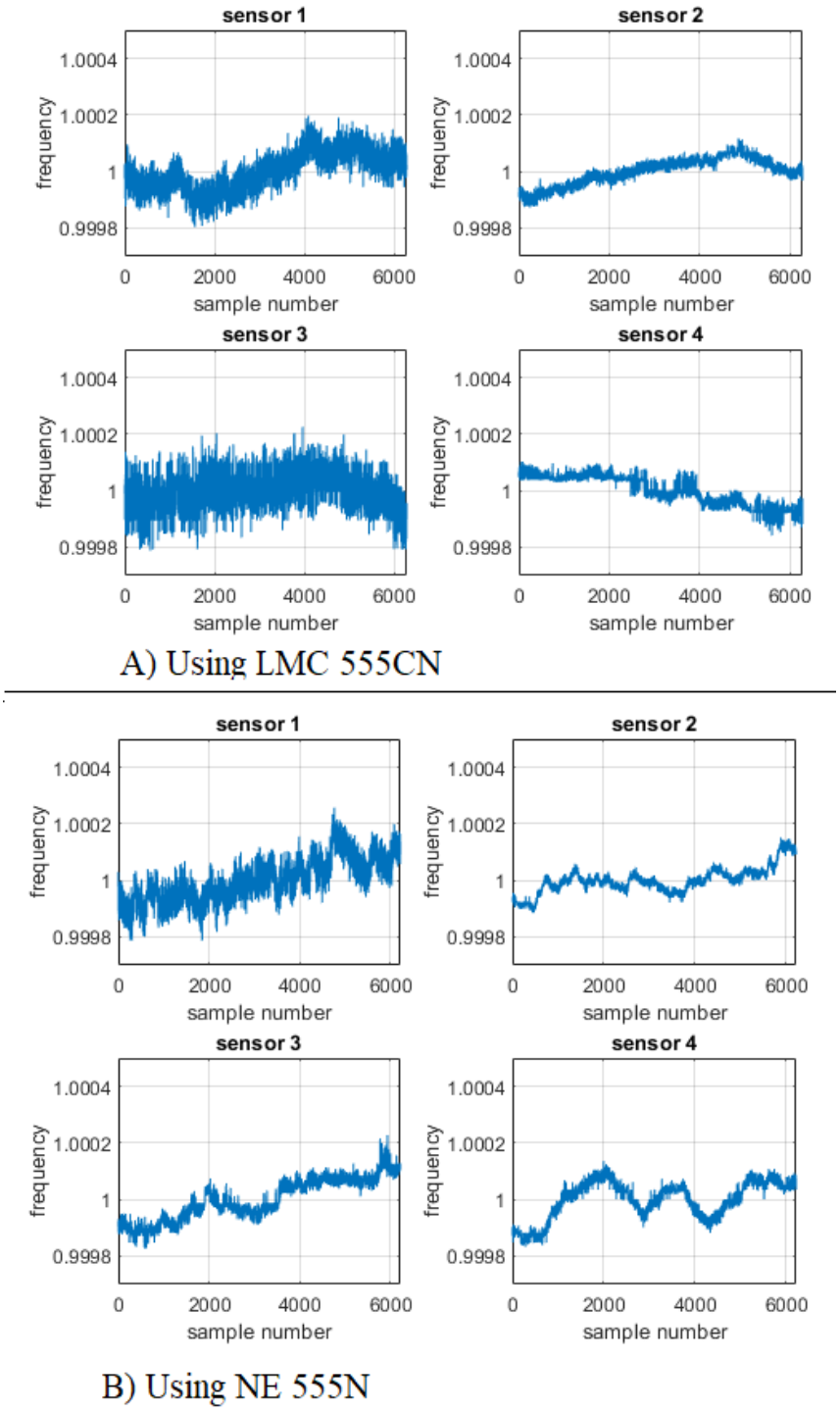

Figure 3.4. Drift acquisition for all four capacitive sensor nodes for several 555 ICs. In the upper part (A) data acquired using LMC 555CN by Texas Instruments, in the bottom part (B) data acquired using NE 555N by ST-Microelectronics

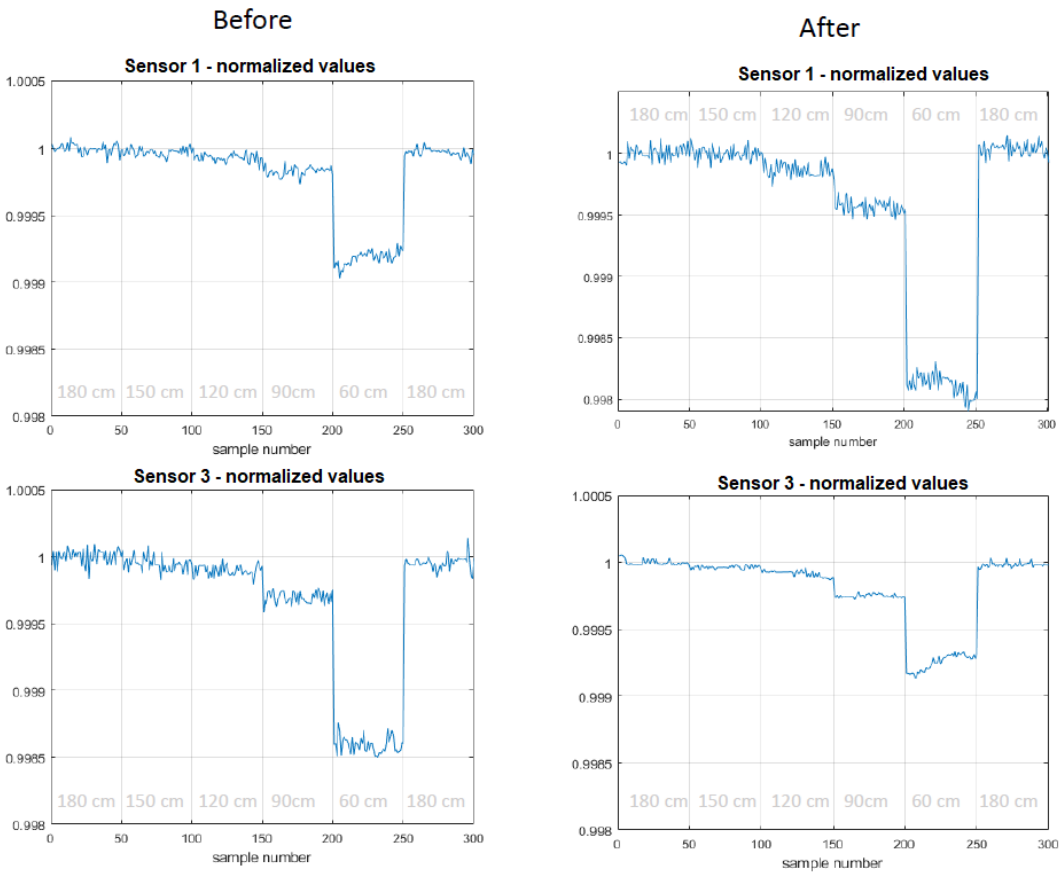

Figure 3.5. Plots of the sensitivity test for sensor nodes 1 and 3 before and after the hardware debugging operations.

3.1.3 Filtering the noise

The obtained signal from this circuit is usually strongly affected by different kinds of ambient noise that could for example come from nearby appliances, electrostatic discharge, temperature and humidity changes. This noise falls in two main categories:

- high-frequency noise from, for example, appliances and light switches;
- a low-frequency drift, that is a DC component that varies much slower than the useful signal component changes. This drift could be attributed to temperature and humidity changes or to slow leak of static charges.

For removing this noise some filtering techniques are used. The output of the sensor node has been sent to both a Median Filter (MF) and a Low-Pass Filter (LPF): with the first the slow drift has been extracted, while with the latter the high-pitch noise has been removed. Then, by simply subtracting median filter output from the LPF output a clean output, without any noise has been obtained. This signal would be the input for the Neural network.

3.2 Ultrasound Sensors System

To provide real-time reference data on the exact position of the person inside the room, and therefore to be able to test the localization system based on capacitive and infrared sensors, an ultrasound sensor system has been used. As already discussed in Section 1.3.5, this kind of sensors guarantee high precision, reliability and low infrastructure costs but makes use of tags for localization. The commercial sensor system used for this project is the one produced by Marvelmind [42] and is depicted in Figure 3.6. It is an off-the-shelf indoor navigation system, designed to provide location data with an accuracy of ± 2 cm. The system is composed of a network of four stationary ultrasonic beacons and a mobile beacon - called HedgHog - installed on objects to be tracked. The beacons are interconnected via radio interface and a modem providing a gateway to the system from PC is also present. The modem is the central controller of the system that is in charge of setting up the system, monitoring it, and interact with the user through the Marvelmind Dashboard software.

The principle of operation is simple: the Time-of-Flight, i.e. the propagation delay, of an ultrasonic pulse between stationary and mobile beacons is calculated and then the position of the mobile beacon is computed using

Figure 3.6. Ultrasound Localization System By Marvelmind. It is composed by a modem and five sensors, among which four are used as stationary reference beacons and one is used as mobile HedgHog beacon [42]

trilateration algorithm. Of course, a direct line of sight among beacons and HedgHog is needed.

The four beacons have been put on the ceiling at a height of 3.05 meters on the angle points of the room, while the HedgHog beacon has been put on a helmet for stability reasons and put on the person to locate. Using a MATLAB script, data from the mobile beacon, provided by the Dashboard have been analyzed.

3.3 Infrared Sensor System

In order to verify the correct behaviour of the D6T infrared thermal sensor, 9-hours temperature measurement has been made in an empty room. To be sure that no one could influence the reading, the sensor was left to take a measurement during an entire night collecting 1 sample every 3 seconds. Together with the infrared sensor, the measurement of the room temperature has been acquired using a temperature and humidity sensor which was located inside the same room. The sensor used was DHT11 Humidity Temperature Sensor that exploits an NTC temperature measurement component [45]. The basic characteristics of DHT11 component are reported in Table 3.1. As can be seen, for the temperature reading it has an accuracy of ± 2°C and a resolution of 1°C.

These values are worse w.r.t. the characteristics of the infrared thermal sensor, that has a temperature resolution (NETD) of 0.14°C and an object temperature output accuracy equal to ± 1.5°C. This means that comparing

Table 3.1. Main characteristics of DHT11 Humidity Temperature Sensor

Item	Measurement Range	Humidity Accuracy	Temperature Accuracy	Resolution	Package
DHT11	20-90% RH 0-50°C	5% RH	±2°C	1	4 Pin Single Row

the data read from the two different sensors this difference in the accuracy and resolution must be taken into account. The difference in temperature between the value read from DHT11 temperature sensor and the average of the reading from the D6T thermal sensor has been computed and the plot of this value over the sample number is reported in Figure 3.7.

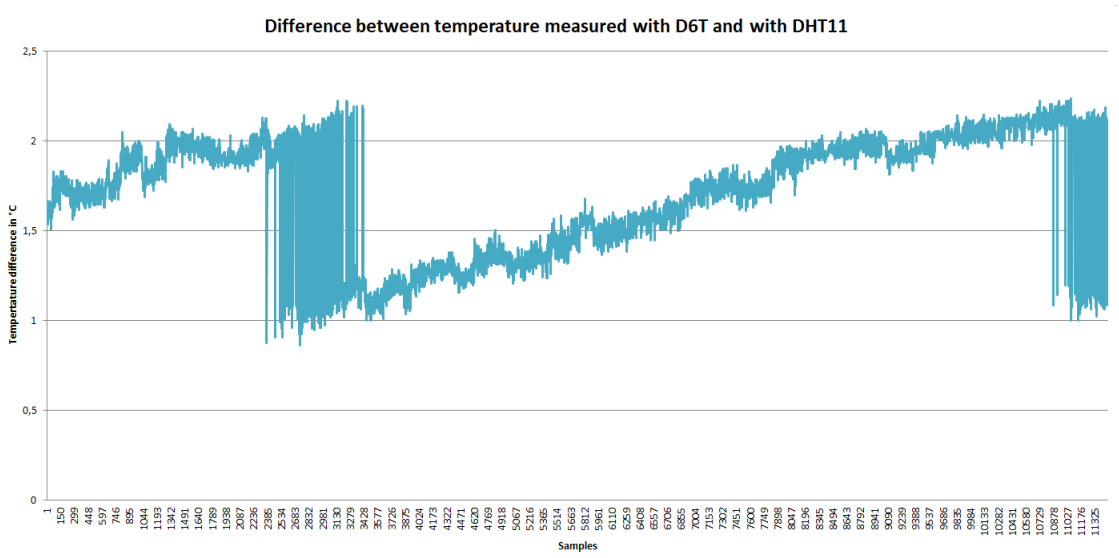

Figure 3.7. D6T thermal sensor stability characterization. Temperature difference between the values read from DHT11 temperature sensor and the average of the readings from the D6T thermal sensor is here plotted. The difference remains in the interval of 1°C , the resolution of DHT11

As can be seen, there is at least 1°C of difference between the two sensors, probably due to the different positions of the sensors in the room or due to the different accuracy. Moreover, the values remain in the interval of 1°C, that is the resolution of the DHT11 sensor. While the ambient temperature was decreasing over the night, the value measured by the D6T decreased too and the difference with the value measured by the DHT11 sensor was

increasing, as shown in the drift present in the plot. Then, at the end of the drift, when also the DHT11 changed its value, the difference returns to be at 1°C.

3.3.1 Infrared sensor: area of sensing evaluation

The room of the experiment is 3.05 meters high and the infrared sensor has been put at the ceiling level. With this information, the infrared sensor field of view at different heights can be easily computed using some geometrical formulas. The field of view of the infrared sensor can be seen, for each direction, as an isosceles triangle where the height is the distance from the sensor and the angle opposite to the base that is the angle of view given by the D6T datasheet. Referring to Figure 3.8, the following formulas can be exploited, knowing α and h, in order to obtain the base a.

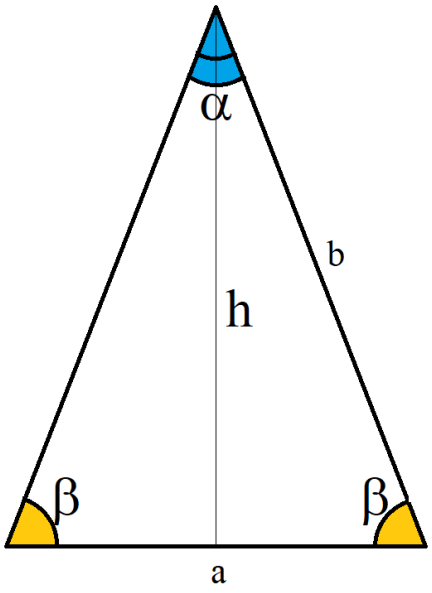

Figure 3.8. Infrared sensor field of view evaluation

$$\beta = \frac{180 - \alpha}{2} \tag{3.2}$$

$$h = \frac{a}{2}\tan(\beta) \tag{3.3}$$

The variables that will be used from now on to compute the field of view of the sensor are shown in Figure 3.9.

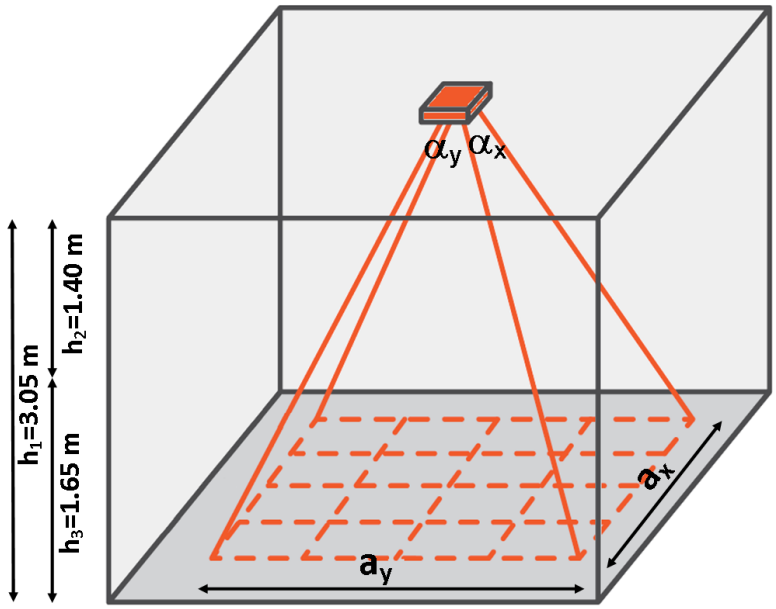

Figure 3.9. Values used for the field of view computation referred to the room. In the figure, h_1 is the distance between the sensor and the floor, h_2 is the distance between the sensor and a person that is $h_3 = 1.65$ m tall. The angle of view α_x and α_x and the corresponding projection on the floor$a_y$and $a_x$are also highlighted.

Along x direction, with α_x= 44.2°, and $h_1 = 3.05m$, the maximum covered area is:

$$a_x = \frac{2 \cdot h_1}{\tan(\beta_x)} = 2.48m \tag{3.4}$$

Along y direction, with α_y= 45.7°, and $h_1 = 3.05m$, the maximum covered area is

$$a_y = \frac{2 \cdot h_1}{\tan(\beta_y)} = 2.57m \tag{3.5}$$

In this way the sensor covers a surface on the floor that is slightly lower than the total area of the room. However, considering that the points of higher sensitivity for the capacitive sensors are the points near the walls

where the capacitive nodes are placed, it is not necessary a higher sensitivity area for the infrared sensor.

Moreover, it must be considered that the part that is better seen by the infrared sensor is the head, both because of proximity and because it is one of the warmest parts of the body usually not covered by clothes. For this reason should be also interesting to consider the field of view not at the floor level but at the head level. Considering that the average height of human is 1.65 m, the same computation has been done with $h_2 = 3.05m - 1.65m = 1.4m$. the obtained results are:

$$a_x = \frac{2 \cdot h_2}{\tan(\beta_x)} = 1.13m \tag{3.6}$$

$$a_y = \frac{2 \cdot h_2}{\tan(\beta_y)} = 1.18m \tag{3.7}$$

This area is about half of the area of sensitivity at the floor level, but it is characterized by a higher resolution since the occupancy ratio of people head in the FOV is higher.

Chapter 4

Data acquisition and Sensor Fusion Results

After the instrumentation has been tested, the acquisition of data has been done. Considering the factors that could positively and negatively influence the reading of the data by the capacitive and infrared sensors, different experiments have been carried out under different conditions. In particular, the experimental data were collected in four experiments by two different people, hereafter will be called User One and User Two. In particular, User One is a male 182 cm tall and was wearing a cotton shirt and denim jeans so that exposed parts of the body were hands neck and head. User Two is a female 163 cm tall wearing cotton T-shirt and cotton trousers so that exposed parts of the body were arms, hands, neck and head. This information is here provided because the taller a person is, the closer the infrared sensor is to his head, therefore, the smaller the field of view area at the height of his head and the greater the precision of measurements from the infrared sensor. Furthermore, the parts not covered by clothing are those which emit the most infrared rays. The use of cotton clothes has been chosen in order to avoid that the reading would be influenced by textile materials which may accumulate electric charge.

Each experiment lasted half an hour. During these experiments, the person was slowly and continuously walking inside the room while all three localization systems were active. The first two experiments (one for each User) were carried out in the evening after sunset, while the other two during the afternoon with the sun's rays penetrating the room through blinds. It was, therefore, possible to test the system under different temperature conditions and with and without the interference of sunlight in the room. In the third

experiment, an element of disturbance to the infrared system has been inserted in order to better test the sensor fusion technique. Since it has been observed that the capacitive sensors have higher drift immediately after they are connected to the power supply and that after some time they arrive in a more stable state, all experiments were carried out after leaving the capacitive sensors on for at least half an hour. All the collected data will be commented in the next sections.

4.1 Experiments one and two - Evening

The first two experiments have been made during the evening by both Users and each of them lasted 30 minutes. In the first experiment User One was walking inside the room following some specific and repeated patterns. A graph of the data from the ultrasound system can be seen in Figure 4.1.

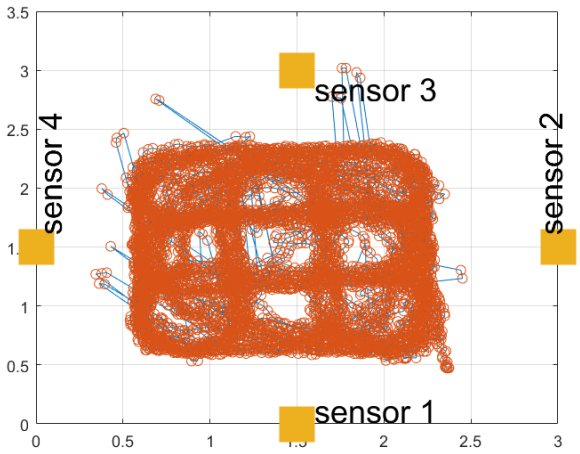

Figure 4.1. Plot of the raw data acquired in Experiment 1 from the ultrasound sensors system

As can be seen, some spikes are present in the reading so it has been necessary to filter them out. In particular, the Hampel Filter function of MATLAB has been used to detect and remove outliers to both the data of x axis and y axis. This filter computes the median of a window of k neighbour samples for each sample of the dataset. It estimates also the standard deviation of each sample about its window median using the median absolute deviation. If a sample differs from the median by more than n_sigma standard deviations, it is replaced with the median. The filter has been applied two times, the

first time with a high value of k= 25 and n_sigma= 2 in order to remove the very high spikes, the second time with a smaller window (k= 10 and n_sigma= 1) in order to smooth remaining data. These values have been set after some tries, looking at the combination of value that could improve the data without removing useful information. The obtained result is in Figure 4.2.

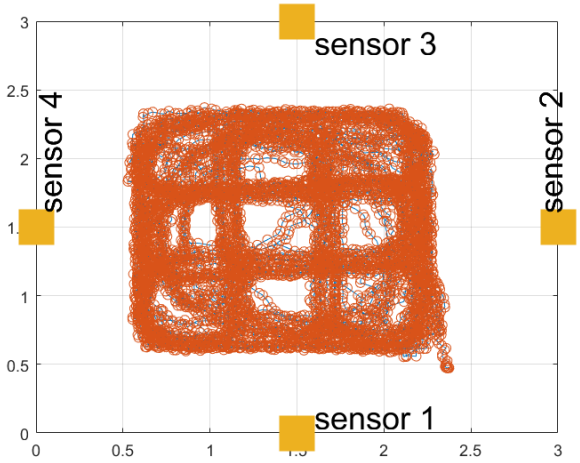

Figure 4.2. Plot of the data acquired in Experiment 1 from the ultrasound sensors system after filtering them with Hampel filter

As it can be seen from the image, this data-set does not cover all the spots of the room, so in the subsequent experiments, a more random direction of walking has been used, trying to cover the whole surface of the room.

The normalized data from the capacitive sensor are present in Figure 4.3. For sensor one some steps that are not related to the movement are present. The same can be observed at the beginning of the acquisition in sensor four. This can be due to the condition of the room, some electric devices that were near sensor one during the execution of the experiment or some faults on the sensors.

The second experiment has been taken in the same evening, with the same conditions, but by User two, in order to test if with a different user the interference seen would have been the same. With respect to the previous experiment, efforts have been made to cover every spot of the floor going in a direction parallel to x and y axis, in diagonal and also in a random way. The filtered data plot from the ultrasound system can be observed in Figure 4.4.

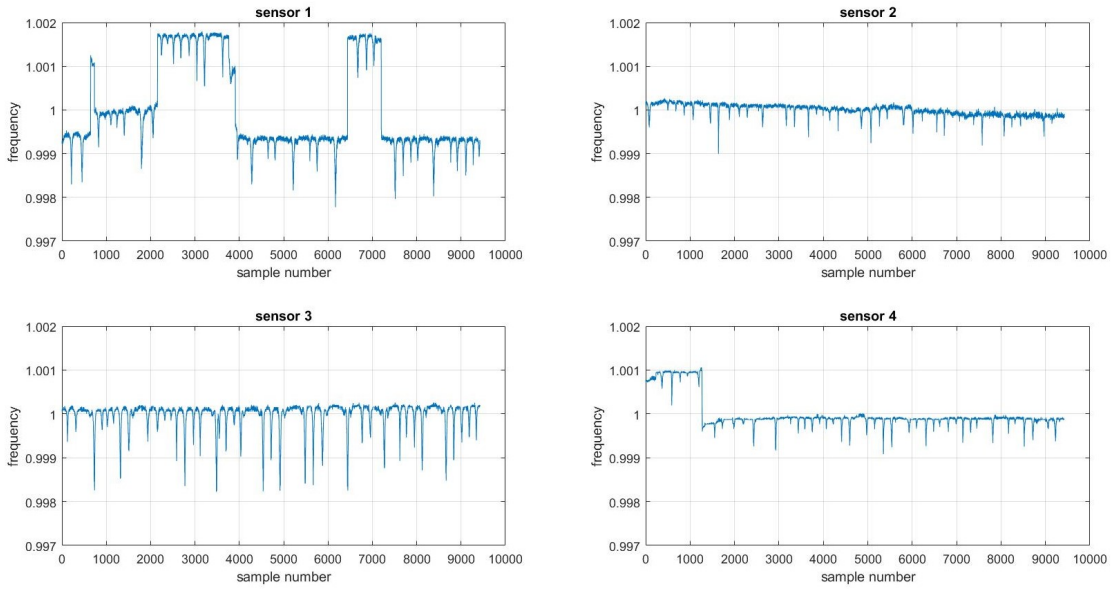

Figure 4.3. Plot of the data acquired in Experiment 1 from the capacitive sensors system

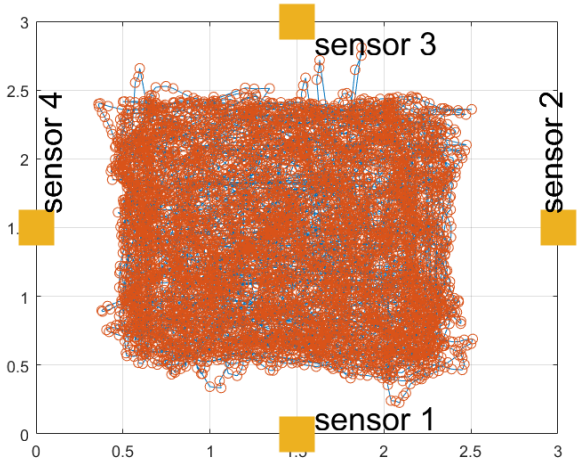

Figure 4.4. Plot of the data acquired in Experiment 2 from the ultrasound sensors system after filtering them with Hampel filter

From the image, it is not possible to see the full path followed during the experiment but it is indicative of the coverage of the room. The data acquired from the capacitive sensor are presented in Figure 4.5.

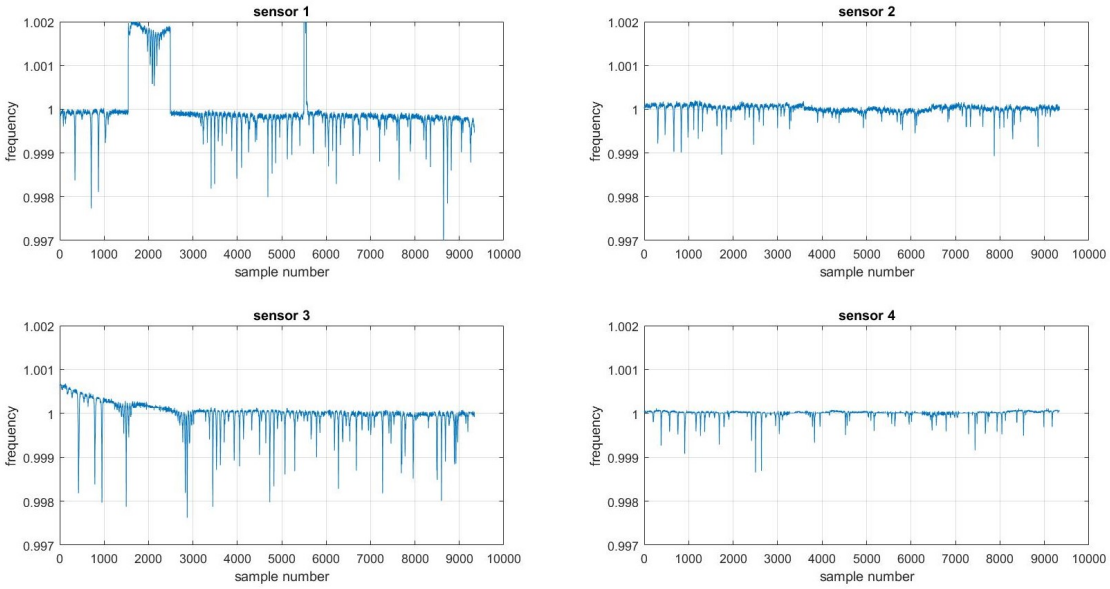

Figure 4.5. Plot of the data acquired in Experiment 2 from the capacitive sensors system

The data from sensor one presents the same shifts as in experiment one so it does not depend on the user or on the clothes he was wearing. Notice that nothing has been changed in the room or around the room when the measurements have been repeated for the other two experiments the day after, but this behaviour did not appear during the other experiments, so it could be due to external, not controllable sources of noise. Drift at the beginning of acquisition by sensor 3 can also be observed, but it can be removed with the technique illustrated in Section 3.1.3.

The data from the infrared sensor for both the experiments are not affected by noise and the difference of temperature between the human and the background reported by the infrared sensor is around 4°C, as it can be seen from Figure 4.6, where some of the data from the first experiment are compared with ground truth in the room.

The difference in temperature is high because the experiment has been done during the evening so the ambient temperature is much lower than the user temperature. However when the human moves across pixel boundaries the sensor reports a lower body temperature since it is divided between multiple pixels. In this way, the difference in temperature between the body and the background gets lower but it is still possible to recognize the position of

the person.

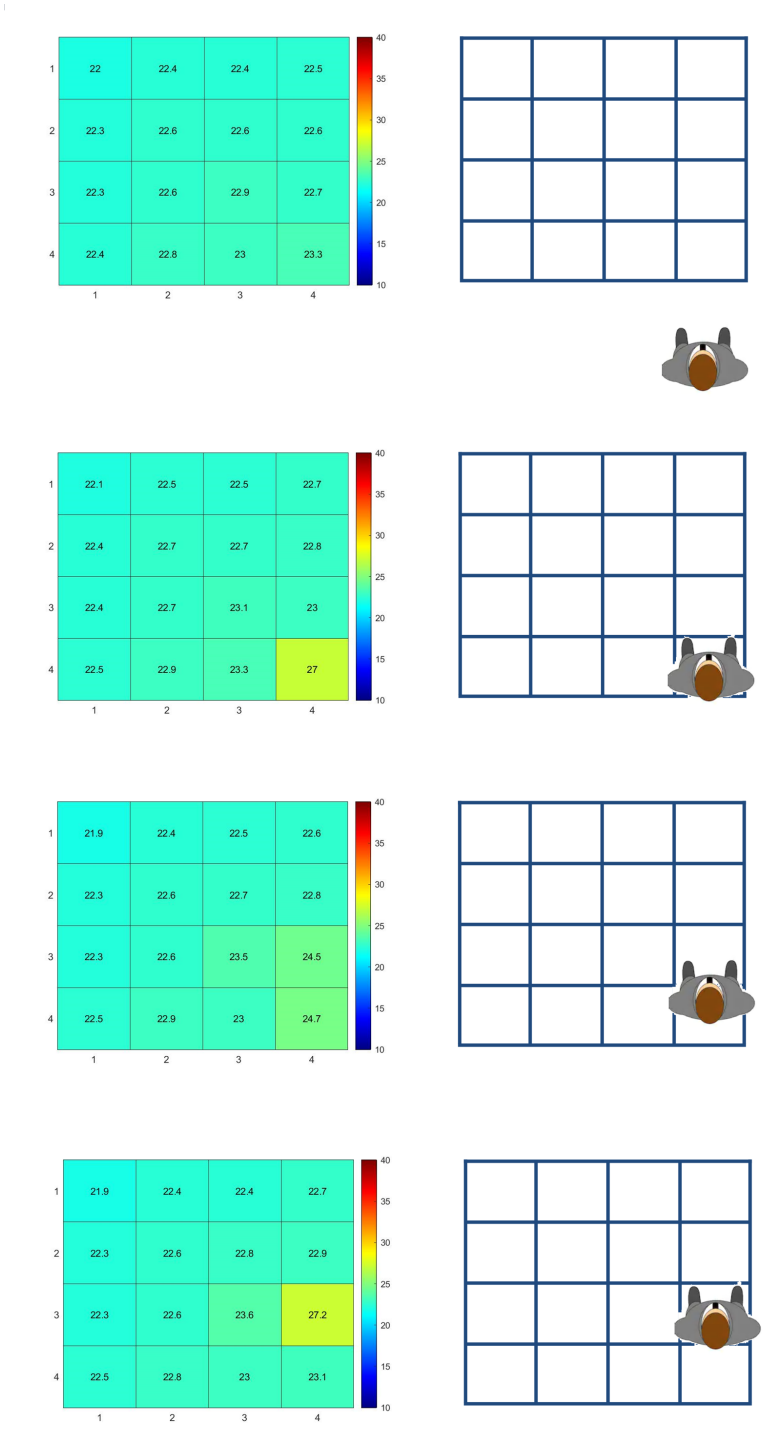

Figure 4.6. Images from the infrared sensor during Experiment 1 and comparison with a schematic showing the ground truth. From the top to the bottom the images are in chronological order

4.2 Experiments three and four - Afternoon

The same experiment has been repeated the day after. What changed was the time at which the experiment has been made, in the afternoon on a sunny day when the sunlight could give some noises to both the infrared and capacitive sensors. In fact, the higher temperature of the room reduced the difference of temperature between the user and the background and this could be a problem for the infrared sensor. Moreover, the sensor components are affected by thermal drift.

In the Experiment number three, an additional source of error for the infrared sensor has been added: a bottle of hot water has been left on the floor in a spot of the room while the User One was walking around the room. Of course, the presence of the bottle has not been sensed by the ultrasound and by the capacitive sensors but has been reported by the infrared as a hotter point w.r.t. the background. This has been made to test if the complete system would understand that the hot object on the floor was not a person or it would give a wrong result, as the infrared sensor system would do if it was alone. In Figure 4.7 the plot of the data acquired in Experiment three from the ultrasound sensors system after applying the Hampel filter. As can be seen, most of the room has been covered during the 30 minutes of walking.

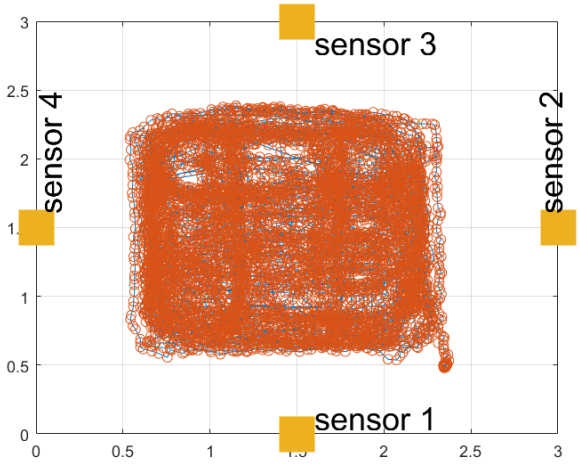

Figure 4.7. Plot of the data acquired in Experiment three from the Ultrasound sensors system after filtering them with Hampel filter

In Figure 4.8 the data from the capacitive sensors system. In the plot relative to Sensor four it is possible to observe that at a certain point a drift

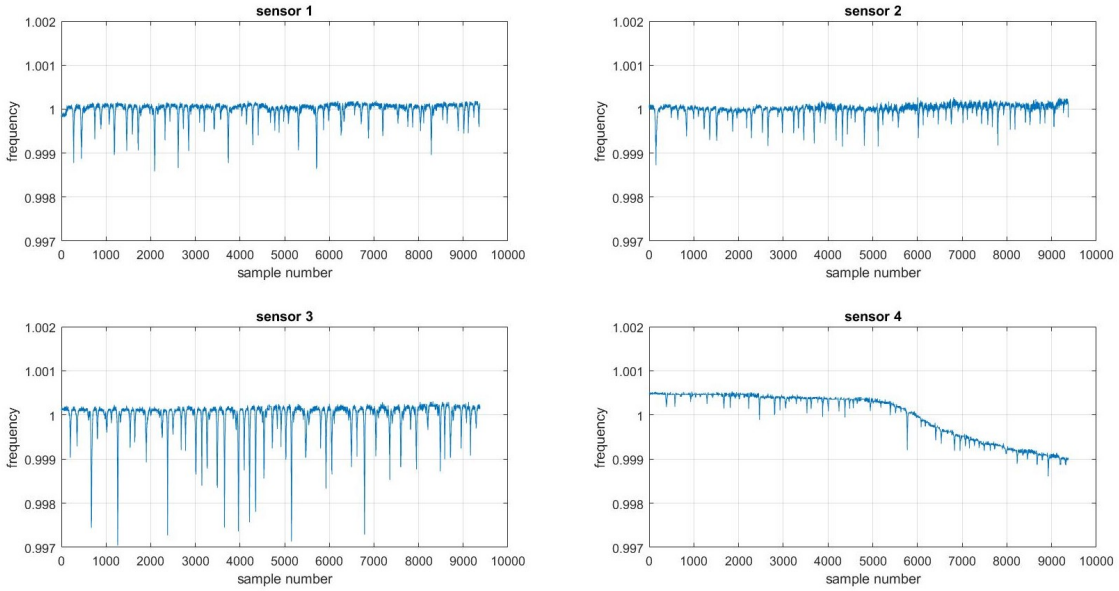

Figure 4.8. Plot of the data acquired in Experiment 3 from the capacitive sensors system

gives the reading a decreasing trend. This can be explained by the fact that at that point of the experiment the sunlight entered in the blinds hitting directly the plate of sensor node four. Except for this deviation, the data set appears to be less noisy than the day before. Some images taken from the reading of the infrared sensor are in Figure 4.9 where also a schematic of the actual situation of the room is present. As can be seen, the reading is influenced by sunlight. In fact, the pixels in the upper right part of each data matrix are at a higher temperature w.r.t. the ones at the bottom left because the sun was hitting that part of the room and not the other. Moreover, it is possible to spot the presence of the hot water bottle that is detected to have a slightly higher temperature than the background. Actually, the real temperature of the water was significantly higher than the room temperature but since the distance from the sensor is around three meters and the bottle of water was small with respect to the total field of view, temperature perceived by the infrared sensor was averaged with the background. The temperature detected by the sensor for the human is about 2°C higher than the hot water but, when the human passes in a region of the room that is among two or more pixels, the detected temperature for the human is comparable with the one of hot water.

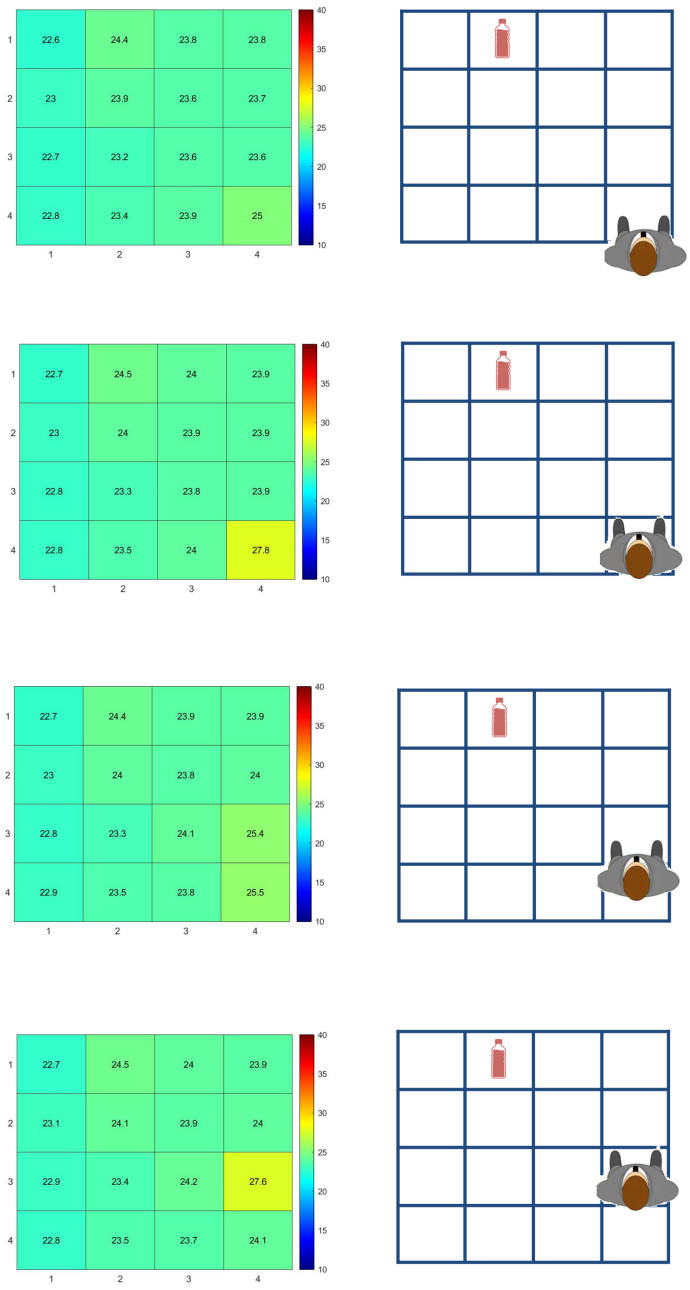

Figure 4.9. Plot of the data acquired in Experiment 4 from the infrared sensors and comparison with ground truth. From the top to the bottom, the images are in chronological order

The last experiment has been made without the hot object on the floor, only User 2 was in the room walking both following some pats and going

in a random way. The experiment has been done shortly after the third one but the curtains have been lowered so as to prevent the light from directly hitting the sensors, having already ascertained in experiment three the effect it has on the various sensors. The sunlight still heating the room, making the difference in temperature between the person and the background less evident compared to the experiment carried out during the evening before. An image from the infrared sensor system acquisition data set is in Figure 4.10. As can be seen, the difference in the detected temperature between human body and background is around 2°C.

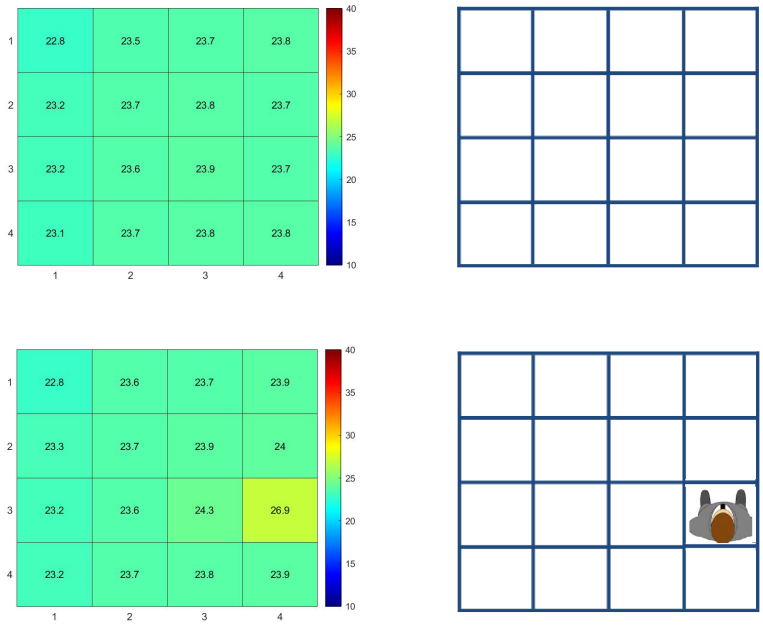

Figure 4.10. Two samples acquired in Experiment 4 from the infrared sensors system. In the upper image the room was empty, in the bottom one there was a person in the position indicated by the scheme

The filtered output data from ultrasound sensors are plotted in Figure 4.11, where it is possible to notice that the room has been fully covered during the experiment using random and non-random patterns.

The normalized data from the capacitive sensors in Figure 4.12. As can be seen, this data set is less affected by drift noise w.r.t. the previous acquisition.

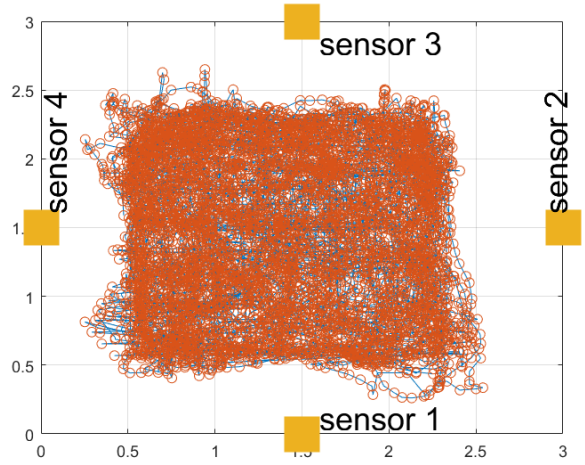

Figure 4.11. Plot of the data acquired in Experiment four from the ultrasound sensors system after filtering them with Hampel filter

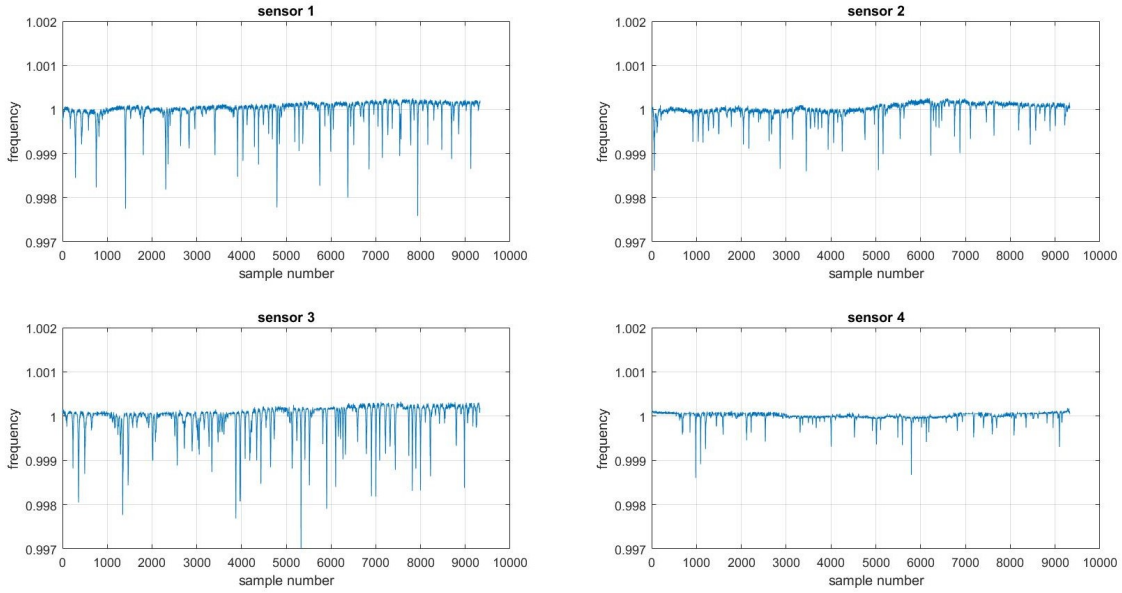

Figure 4.12. Plot of the data acquired in Experiment 4 from the capacitive sensors system

4.3 Experimental data merging

Data from the three sensor systems have been acquired simultaneously, with approximately the same start and stop times, for exactly the same amount of time. However, they were acquired by three separate systems, each with its sampling rate which can, depending on the case, be lower or higher than the expected one based on problems encountered or not during the communication phase. Therefore, in order to have a data-set with the same sampling rate and referred to the same timestamps, the following approach has been used:

- The data were sampled by the various sensors with the highest sampling rate that could be obtained without errors from each type: 8 Hz for the infrared sensor, 5 Hz for the capacitive sensors and 3.5 Hz for the ultrasound sensor. During the acquisition phase, the timestamp related to the acquired data has been saved. Although the systems communicated with different computers, since all the computers on which the MATLAB scripts ran were connected to the same internet network, the time reference, given by the web, is the same for each system.

- After the acquisition, data from all sensors have been checked to verify that the start and stop moments were common to all three. If not, some samples have been discarded in order to have the same interval for all the sensors.

- A vector of timestamps evenly spaced over the specified interval has been obtained using the linspace() function of MATLAB. Then, using linear interpolation, the data from the three systems have been resampled at the exact time present in the vector of timestamps obtained. The final sampling frequency has been in this way set to 5 Hz. The MATLAB function interp1() has been used for making the interpolation, generating the missing samples for each timestamp.

The data have been saved in a CSV file reporting for each row the data from all the sensors and a unique timestamp. It consists of 23 column matrix (with rows depending on the number of samples obtained during the experiment). Four columns correspond to the four capacitive sensors. Sixteen columns contain the data obtained from the IR sensor, and the last two columns contain X and Y axis information obtained from the ultrasound sensor. This file will be the input file of a Neural Network that will analyze

the data and obtain the best model to identify the final position of a person in the room.

Chapter 5

Conclusion and future work

A sensor fusion technique between an infrared thermal sensor and a capacitive sensors system was applied to an indoor location system to be used in smart homes and assisted living environments.

Analyzing the two systems separately it can be seen how their strengths and weaknesses have been perfectly balanced with the sensor fusion approach.

The capacitive sensor method applied in the localization field can bring many advantages since it is tag-less, unobtrusive and privacy-aware. The installation is easy since plates can be attached on the wall and can be hidden behind some covers and become invisible and unobtrusive for the users. Moreover, it is cheap both because of the material it is made of and because of the low power consumption during the usage. The main problem with this kind of sensor is the sensitivity that changes with the distance. This leads to a low sensitivity area in the middle of the room if only capacitive sensors are used. Moreover, they are affected by different sources of noise that cannot be easily controlled. Above all drift affects most this kind of sensor.

The infrared thermal sensor suits well the purpose of indoor human localization because it acquires images of the situation in the room without violating the privacy of the user. It is tag-less and unobtrusive and does not need a big effort to install it. However, it has uneven sensitivity: when a human passes through the area covered by two different pixels the temperature value sensed is less than the temperature sensed when the human occupies the area covered by a pixel alone. Moreover considering 3 meters as the standard height of a room's ceiling, the floor area covered by an infrared sensor with the same sensitivity of the one used in this work, is around 2.5 m x 2.5

m, that means the border of a standard 3 m x 3 m room is not covered. Merging the data of the two sensing systems can create a much more accurate, sensitive and robust system:

- Capacitive drift can be corrected by the use of a sensor like the infrared one that is not affected by the same problem;
- The overall sensitivity range can be extended for both the systems: the lack of sensitivity of the infrared sensor at the borders of the room are balanced by the high sensitivity of the capacitive sensors in the proximity of the walls. In the same way, the lack of sensitivity of the capacitive sensors in the middle point of the room is compensated by the field of view area of the infrared one. In the parts where both systems have good sensitivity, the infrared non-homogeneous sensitivity when crossing pixels can be corrected by the capacitive ones.
- Infrared sensor parallax errors can be corrected by the capacitive sensor.

In conclusion, the sensor fusion approach can lead to an improvement in the system. In fact, robustness and reliability are increased by adding redundancy, spatial and temporal coverage are extended and resolution and uncertainty are improved.

To check the improvement obtained, it will be necessary to analyze the data through Neural Networks.

Should be compared the localization performance using first the data-set composed by data from only capacitive sensors, then only data from infrared sensors and at last a merge of the two systems. In this way, it will be clear in terms of accuracy and error the actual improvement that the sensor fusion can give to both the systems.

It will be possible to see if the errors and drifts from one of the two sides will be actually recognized in the overall system. For example, using the data-set obtained from the Experiment three it will be possible to see if the hot water bottle placed in the room during the experiment and sensed by the infrared sensor will be recognized as the presence of a person or if the capacitive sensor contributes will avoid this error.

Further improvements can be implemented in future work:

- The capacitive sensor system could be optimized both in hardware components and in processing techniques in order to reduce drift and noise level. This could lead to more accurate measurement and could also speed up the system by allowing to make the method applicable to more

realistic and dynamic contexts. Some improvements could also be done to reduce the power consumption for long-term service using either battery or wireless power.

- Regarding the infrared sensor system, the Arduino board used for collecting and sending data from the sensor to the computer can be replaced with a customized circuit containing a microcontroller IC and an Xbee module. This would reduce the size of the system and improve the performances.
- The size of the experimental room could be increased beyond 3 m x 3 m: the number of capacitive plates and infrared sensors could be increased in order to cover a bigger space and other sensors positioning strategies could be tested.

During this work, a lot of effort has been made to make everything work in the best way and to try to have a scientific approach to the problems encountered. The expectation is that this system will be enhanced to be ready and available to improve the lives of users, especially those who need care and assistance.

Appendix A

Microcontroller code

A.1 Transmitter

The code used for the trasmission of data from the infrared sensor is here reported.

```
#include <Wire.h>
#include <WireExt.h>
#define D6T_addr 0x0A // Address of OMRON D6T is 0x0A in hex
#define D6T_cmd 0x4C // Standard command is 4C in hex

/*-------------------------------*/

#include <XBee.h>
XBee xbee = XBee();
uint8_t payload[33] ; //  bytes to be transmitted via radio
uint8_t frameId = NO_RESPONSE_FRAME_ID;  // xbee variable inizialization
uint8_t option = DISABLE_ACK_OPTION;
Tx16Request tx = Tx16Request(0xDCBA, option, payload, sizeof(payload), frameId);
uint16_t frq;

/*-------------------------------*/

const long period = 333;
unsigned long start = millis();
int counter;
 uint8_t  rbuf[35]; // 35 bytes coming from the sensor.
uint8_t valid_byte;
int tdata[16]; // The data coming from the sensor is 16 elements, in a 16x1 array
int tPTAT; //mean value of temperature
int tPEC; // crc value from the sensor
uint16_t value[16];
unsigned char crc;
double temp;

int i;
int MAXREADS=3;
```

```
//------------------start--------------------------

void setup()
{
    Wire.begin();
    Serial.begin(9600);
    xbee.setSerial(Serial);
    pinMode(13, OUTPUT);
}

void loop()
{
    start = millis();// save the information about the starting time of transmission

    //digitalWrite(13, 0);

    valid_byte=0;

for (i = 0; i < 35; i++)
          {
              rbuf[i] = 0;
          }

//-------------------------communication and reading of data from d6t sensor----------------
     Wire.beginTransmission(D6T_addr);
     Wire.write(D6T_cmd);
     Wire.endTransmission();

     if (WireExt.beginReception(D6T_addr) >= 0)
     {
       i = 0;
          for (i = 0; i < 35; i++)
          {
              rbuf[i] = WireExt.get_byte(); //read the data from the sensor
          }
       WireExt.endReception();
     }

   //-------------------------------------------------------------------------------------------


  // ----------------------crc calculation-----------------------


  crc= calc_crc(0x15);
  for (i = 0; i < 34; i++)
  {
    crc=calc_crc(rbuf[i] ^ crc);

  }
    tPEC= rbuf[34];


 // ------------------------------------------------------------
```

```
//If the so computed crc does not match the tPEC repeat the reading for a maximum of 3 times


  for (counter = 0; (counter < MAXREADS) & (crc != tPEC); counter++)
  {
        //while (counter>0 & (crc!= tPEC)){
        //Serial.print("ERRORE, prova di rilettura dei dati. Valore di counter:\n");
        //Serial.print(counter);

      if (WireExt.beginReception(D6T_addr) >= 0)
      {
           i = 0;
            for (i = 0; i < 35; i++)
            {
              rbuf[i] = WireExt.get_byte();
            }
          WireExt.endReception();
      }



      crc= calc_crc(0x15);
      for (i = 0; i < 34; i++)
       {
        crc=calc_crc(rbuf[i] ^ crc);

        }
      tPEC= rbuf[34];

   }


  if(crc== tPEC)
  {valid_byte=1;}
 //-----------------------------------------------------------------------



    tPTAT = (rbuf[0]+(rbuf[1]<<8));  //mean value of temperature, not used

  //--------------conversion from bytes to 16 words------------------------

    for (i = 0; i < 16; i++)
          {
             tdata[i]=(rbuf[(i*2+2)]+(rbuf[(i*2+3)]<<8));
              value[i]=tdata[i] /* * 0.1*/;
          }

 //-------------------------------------------------------------------------------



 //------------------------------sending of data via xbee----------------------
     for (i=0; i<16; i++)
     {
      frq=value[i];
```

```
      payload[i*2] = highByte(frq);
      payload[i*2+1] = lowByte(frq);


     }
     payload[32]=valid_byte;

    xbee.send(tx);


//-------------------------------------------------------------------------------------------



//----------------if the interval of time of 333ms is not elapsed wait-------------------


   while (millis() < start + period){
       }

//-------------------------------------------------------------------------------------

       //digitalWrite(13, 1);
}

//-----------------------------------the end-----------------------


//------------------------------crc calculation function-------------------------
unsigned char calc_crc(unsigned char data)
{int index;
 unsigned char temp;
    for(index=0;index<8;index++)
    {
        temp= data;
        data <<= 1;
            if(temp & 0x80)
            {
                data ^= 0x07;
            }
    }
 return data;
}
```

A.2 Receiver

The arduino code used for the reception of data via radio is here reported.

```
#define highWord(w) ((w) >> 16)
#define lowWord(w) ((w) & 0xffff)
#define makeLong(hi, low) (((long) hi) << 16 | (low))

#include <XBee.h>

XBee xbee = XBee();
XBeeResponse response = XBeeResponse();
//response objects for responses we expect to handle
Rx16Response rx16 = Rx16Response();


uint8_t rec_data[32];
uint16_t add;
uint8_t check_error;
 uint16_t value[16];

int i;
String address_frq;


void setup() {

  // start serial
  Serial.begin(9600);
  xbee.setSerial(Serial);


}

// continuously reads packets, looking for RX16 or RX64
void loop() {

    xbee.readPacket();

    if (xbee.getResponse().isAvailable()) {
      // got something

        if (xbee.getResponse().getApiId() == RX_16_RESPONSE) {
                xbee.getResponse().getRx16Response(rx16);
                check_error = rx16.getErrorCode();
                if (check_error == NO_ERROR) {

                     add = rx16.getRemoteAddress16();
                      String add_str = String(add, HEX);



                      for (i=0; i<16; i++)
                     {
                       rec_data[i*2]  = rx16.getData(i*2);
                        rec_data[i*2+1]  = rx16.getData(i*2+1);
                       value[i]=(rec_data[(i*2+1)]+(rec_data[(i*2)]<<8));
                      Serial.println(  value[i]);
```

```
                    }
                 rec_data[32] = rx16.getData(32);
                Serial.println(  rec_data[32]);// valid byte

            }
        }
    }
}
```

Appendix B

MATLAB code

B.1 Acquisition of the data through serial port

```
clear all;
times_to_run=180;
time_vector = zeros(times_to_run,1);
Data=zeros(times_to_run, 16);
valid_byte=zeros(times_to_run, 1);
temperature_dht11=zeros(times_to_run, 1);
MATRIX=zeros(4,4);
counter=0;
minutes_to_run=1;
end_time= minutes_to_run *60;
%%%%%%%%%%%%%%%%%%%%%%%%%%%%%%%%%%%%%%%%

serialPort = 'COM5';
s = serial(serialPort);
set(s,'BaudRate',9600);
fopen(s);

%%%%%%%%%%%%%%%%%%%%%%%%%%%%%%%%%%%%%%%%

start_time= tic;
while(toc(start_time)< end_time )
counter= counter+1;
    for i=1:16
    arduino(i) = fscanf(s, '%f \n'); %Read Data from Serial as String


    end

   valid_byte(counter)=fscanf(s, '%f\n ');
time_vector(counter) =now;

Data(counter, :)= arduino;

end

fclose(instrfind);
```

```
Time_Stamp = datetime(time_vector,'ConvertFrom','datenum','Format','d-MMM-y HH:mm:ss:SSS');

T= table( Data *0.1, Time_Stamp, valid_byte);
T2= table( Data*0.1 , time_vector, valid_byte);

writetable(T,'./infrared_output_date_time.csv');
writetable(T2,'./infrared_output.csv');

%%%%%%%%%%%%%%%%%%%%%%%%%%%%%%%%%%%%%%%%
```

B.2 Data plotting

```
clear all;
MATRIX=zeros(4,4);
counter=0;
T = readtable('./infrared_output.csv');
toDelete = T.valid_byte <1;
T(toDelete,:) = [];
[times_to_run, col]=size(T);
Data(:,:)= T(:, 1: end-2).Variables;
writetable(T(:, 1: end),'./infrared_output_validbit.csv');
mkdir images;
for counter=1:times_to_run
     for i=1:4
        for j=1:4
            index=(i)+4*(j-1);
    MATRIX (j, i)=  Data(counter, index);
        end
    end

 heatmap(MATRIX,'ColorMap', jet, 'ColorLimits', [10, 40]);

 saveas(gcf,sprintf('./images/infrared_%05d',counter),'jpg');

end
```

Bibliography

[1] S. Shukri, L. Munirah Kamarudin, and M. Hafiz Fazalul Rahiman, 'Device-Free Localization for Human Activity Monitoring', in Intelligent Video Surveillance, A. J. R. Neves, Ed. IntechOpen, 2019.

[2] T. Kivimäki, T. Vuorela, P. Peltola, and J. Vanhala, 'A Review on Device-Free Passive Indoor Positioning Methods', IJSH, vol. 8, no. 1, pp. 71–94, Jan. 2014, doi: 10.14257/ijsh.2014.8.1.09.

[3] T. B. Moeslund and E. Granum, 'A Survey of Computer Vision-Based Human Motion Capture', Computer Vision and Image Understanding, vol. 81, no. 3, pp. 231–268, Mar. 2001, doi: 10.1006/cviu.2000.0897.

[4] Imen Jegham, Anouar Ben Khalifa, Ihsen Alouani, Mohamed Ali Mahjoub, "Vision-based human action recognition: An overview and real world challenges", Forensic Science International: Digital Investigation, Volume 32, 2020, 200901,ISSN 2666-2817, https://doi.org/10.1016/j.fsidi.2019.200901.

[5] D. Hauschildt and N. Kirchhof, Advances in thermal infrared localization: Challenges and solutions Int. Conf. Indoor Positioning and Indoor Navigation, (2010), pp. 1-8.

[6] Hsu, Hui-Huang Peng, W.-J Shih, Timothy Pai, Tun-Wen Man, Ka. (2015). Smartphone Indoor Localization with Accelerometer and Gyroscope. Proceedings - 2014 International Conference on Network-Based Information Systems, NBiS 2014. 465-469. 10.1109/NBiS.2014.72.

[7] C. Hsu and C. Yu, "An Accelerometer Based Approach for Indoor Localization," 2009 Symposia and Workshops on Ubiquitous, Autonomic and Trusted Computing, Brisbane, QLD, 2009, pp. 223-227. doi: 10.1109/UIC-ATC.2009.90

[8] Scott J., Dragovic B. (2005) Audio Location: Accurate Low-Cost Location Sensing. In: Gellersen H.W., Want R., Schmidt A. (eds) Pervasive Computing. Pervasive 2005. Lecture Notes in Computer Science, vol 3468. Springer, Berlin, Heidelberg

[9] X. Bian, G. Abowd and J. Rehg, Using sound source localization in a home environment Pervasive Computing, ser. Lecture Notes in Computer Science, H. Gellersen, R. Want, and A. Schmidt, Eds. Springer, Berlin, (2005), pp. 19-36.

[10] Li, Jian Han, Guangjie Zhu, Chunsheng Sun, Guiqing. (2016). An Indoor Ultrasonic Positioning System Based on TOA for Internet of Things. Mobile Information Systems. 2016. 1-10. 10.1155/2016/4502867.

[11] Medina, C.; Segura, J.C.; De la Torre, Á. Ultrasound Indoor Positioning System Based on a Low-Power Wireless Sensor Network Providing Sub-Centimeter Accuracy. Sensors 2013, 13, 3501-3526.

[12] Goswami S. (2013) Radio Frequency Positioning. In: Indoor Location Technologies. Springer, New York, NY

[13] El-Kafrawy K, Youssef M, El-Keyi A. Impact of the human motion on the variance of the received signal strength of wireless links. In: Proceeding of IEEE 22nd International Symposium on Personal Indoor and Mobile Radio Communications (PIMRC'11); 11–14 September 2011; Toronto, ON, Canada. IEEE; 2012. pp. 1208-1212

[14] iF. Zafari, A. Gkelias and K. K. Leung, "A Survey of Indoor Localization Systems and Technologies," in IEEE Communications Surveys Tutorials, vol. 21, no. 3, pp. 2568-2599, thirdquarter 2019.

[15] Martin L. Pall, Wi-Fi is an important threat to human health, Environmental Research, Volume 164, 2018,Pages 405-416,ISSN 0013-9351.

[16] L. E. M. Matheus, A. B. Vieira, L. F. M. Vieira, M. A. M. Vieira and O. Gnawali, "Visible Light Communication: Concepts, Applications and Challenges," in IEEE Communications Surveys Tutorials, vol. 21, no. 4, pp. 3204-3237, Fourthquarter 2019. doi: 10.1109/COMST.2019.2913348

[17] Y. Zhuang et al., "A Survey of Positioning Systems Using Visible LED Lights," in IEEE Communications Surveys Tutorials, vol. 20, no. 3, pp. 1963-1988, thirdquarter 2018. doi: 10.1109/COMST.2018.2806558.

[18] J. P. D. Vries, L. Simi´c, A. Achtzehn, M. Petrova, and P. Mähönen,"The Wi-Fi 'congestion crisis': Regulatory criteria for assessing spectrum congestion claims," Telecommun. Policy, vol. 38, nos. 8–9, pp. 838–850, 2014.

[19] Richardson, Bruce Leydon, Krispin Fernström, Mikael Paradiso, Joseph. "Z-tiles: Building blocks for modular, pressure-sensing floorspaces". Proceedings of CHI. 1529-1532. 10.1145/985921.986107. (2004)

[20] R. J. Orr and G. D. Abowd, The smart floor: a mechanism for natural user identification and tracking, Extended Abstracts Human Factors Computing Syst., (2000), pp. 275-276.

[21] D. Savio and T. Ludwig, "Smart Carpet: A Footstep Tracking Interface," 21st International Conference on Advanced Information Networking and Applications Workshops (AINAW'07), Niagara Falls, Ont., 2007, pp. 754-760.

[22] T. Grosse-Puppendahl et al., 'Finding Common Ground: A Survey of Capacitive Sensing in Human-Computer Interaction', in Proceedings of the 2017 CHI Conference on Human Factors in Computing Systems - CHI '17, Denver, Colorado, USA, 2017, pp. 3293–3315, doi: 10.1145/3025453.3025808.

[23] D. Galar and U. Kumar, 'Sensors and Data Acquisition', in eMaintenance, Elsevier, 2017, pp. 1–72.

[24] A. Ramezani Akhmareh, M. Lazarescu, O. Bin Tariq, and L. Lavagno, "A tagless indoor localization system based on capacitive sensing technology," Sensors, vol. 16, no. 9, p. 1448, 2016.

[25] O. B. Tariq, M. T. Lazarescu, J. Iqbal, and L. Lavagno, "Performance of machine learning classifiers for indoor person localization with capacitive sensors," IEEE Access, vol. 5, pp. 12 913–12 926, 2017.

[26] J. Iqbal, A. Arif, O. B. Tariq, M. T. Lazarescu, and L. Lavagno, "A contactless sensor for human body identification using RF absorption signatures," in 2017 IEEE Sensors Applications Symposium (SAS). IEEE, 2017, pp. 1–6.

[27] J. Iqbal, M. T. Lazarescu, O. B. Tariq, and L. Lavagno, "Long range, high sensitivity, low noise capacitive sensor for tagless indoor human localization," in 2017 7th IEEE International Workshop on Advances in Sensors and Interfaces (IWASI), Jun. 2017, pp. 189–194.

[28] J. Iqbal, M. T. Lazarescu, A. Arif, and L. Lavagno, "High sensitivity, low noise front-end for long range capacitive sensors for tagless indoor human localization," in 2017 IEEE 3rd International Forum on Research and Technologies for Society and Industry (RTSI), Sep. 2017, pp. 1–6.

[29] J. Iqbal, M. T. Lazarescu, O. B. Tariq, A. Arif, and L. Lavagno, "Capacitive sensor for tagless remote human identification using body frequency absorption signatures," IEEE Transactions on Instrumentation and Measurement, vol. 67, no. 4, pp. 789–797, Apr. 2018.

[30] O. B. Tariq, M. T. Lazarescu, and L. Lavagno, "Neural network-based indoor tag-less localization using capacitive sensors," in Proceedings of the 2019 ACM International Joint Conference on Pervasive and Ubiquitous Computing and Proceedings of the 2019 ACM International Symposium on Wearable Computers. ACM, 2019, pp. 9–12.

[31] S. D. Gunapala et al., "Quantum Well Infrared Photodetector Technology and Applications," in IEEE Journal of Selected Topics in Quantum Electronics, vol. 20, no. 6, pp. 154-165, Nov.-Dec. 2014, Art no. 3802312.

[32] Hwaiyu Geng, "ELECTRO-OPTICAL INFRARED SENSOR TECHNOLOGIES FOR THE INTERNET OF THINGS," in Internet of Things and Data Analytics Handbook, Wiley, 2017, pp.167-185

[33] J. L. Honorato, I. Spiniak and M. Torres-Torriti, "Human Detection Using Thermopiles," 2008 IEEE Latin American Robotic Symposium, Natal, Rio Grande do Norte, 2008, pp. 151-157.

[34] J. Yun and S.-S. Lee, 'Human Movement Detection and Identification Using Pyroelectric Infrared Sensors', Sensors, vol. 14, no. 5, pp. 8057–8081, May 2014, doi: 10.3390/s140508057.

[35] Omron web site - D6T MEMS Thermal Sensors https://www.components.omron.com/product-detail?partNumber=D6T - Last access February 2020

[36] Omron, MEMS Thermal Sensors User's Manual-D6T https://omronfs.omron.com/en_US/ecb/products/pdf/en_D6T_uses_manual.pdf - Last access February 2020

[37] Omron, MEMS Thermal Sensors D6T catalog https://omronfs.omron.com/en_US/ecb/products/pdf/en_D6T_catalog.pdf - Last access February 2020

[38] 'UM10204 I2C-bus specification and user manual', vol. 2014, p. 64, 2014 https://www.nxp.com/docs/en/user-guide/UM10204.pdf - Last access February 2020

[39] ATmega328P - 8-bit AVR Microcontroller with 32K Bytes In-System Programmable Flash DATASHEET - http://ww1.microchip.com/downloads/en/DeviceDoc/Atmel-7810-Automotive-Microcontrollers-ATmega328P_Datasheet.pdf

[40] 'XBee/XBee-PRO S2C 802.15.4 RF Module', https://www.digi.com/resources/documentation/digidocs/pdfs/90001500.pdf - Last access February 2020

[41] 'XCTU Next Generation Configuration Platform for XBee/RF Solutions', https://www.digi.com/products/embedded-systems/digi-xbee/digi-xbee-tools/xctu#productsupport-utilities - Last access February 2020

[42] Marvelmind Indoor Navigation System Operating manual https://marvelmind.com/pics/marvelmind_navigation_system_manual.pdf - Last access February 2020

[43] Texas Instruments - LMC555 CMOS Timer Datasheet http://www.ti.com/lit/ds/symlink/lmc555.pdf - Last access March 2020

[44] STMicroelectronics NE555- SA555 - SE555 General-purpose single bipolar timers Datasheet https://www.st.com/resource/en/datasheet/cd00000479.pdf- Last access March 2020

[45] DHT11 Technical Data-Sheet https://www.mouser.com/datasheet/2/758/DHT11-Technical-Data-Sheet-Translated-Version-1143054.pdf - Last access March 2020

[46] MathWorks Outlier removal using Hampel identifier https://it.mathworks.com/help/signal/ref/hampel.html - Last access March 2020

[47] Wikipedia - Training, validation, and test sets https://en.wikipedia.org/wiki/Training,_validation,_and_test_sets - Last access March 2020

Acknowledgements

I would like to dedicate this space to people who, with their support, have helped me in the realization of this thesis and during my university career.

A heartfelt thanks to my supervisors Mihai Lazarescu and Luciano Lavagno for their infinite availability, for their indispensable advice and for the knowledge transmitted throughout this thesis work.

Thanks to Osama Bin Tariq for helping and guiding me with practical tips when running the experiments. The long waits hoping that the sensors worked well have been less tedious together.

Thanks to the Politecnico di Torino, for welcoming me and providing the tools and knowledge necessary to train me. Thanks to all the professors I met during my university experience: each of them gave me the opportunity to learn and grow. Among them, a special thank goes to Professor Passerone for his kindness and for giving me the opportunity to see the Politecnico under the starlight.

Thanks to the Polietnico choir which I had the honour of being part of during part of my journey.

Thanks to the course colleagues: we supported, helped and encouraged each other during the long exam sessions. Among these, a heartfelt thanks to the one who most of all had to support and endure me in recent years, Nicoletta. In you, I found a good colleague and friend. Thanks also to the new friends met in Turin and to the old friends spread all over the world. In particular I would like to thank my bachelor degree friends for being present despite the distance.

Last but not least, I would like to thank my family and Giuseppe who have always been by my side, often not physically but with the heart, in good and bad times. Without your support, I would never have come to this point. Thanks for being an inexhaustible source of love, support and joy.